X-Ray Polarimetry and Cadmium Zinc Telluride (CZT) Detectors

M. Beilicke, Q. Guo, F. Kislat, K. Lee, J. Martin, H. Krawczynski (Wash. Univ.),

A. Burger, M. Groza (Fisk Univ.), J. Matteson (UCSD)

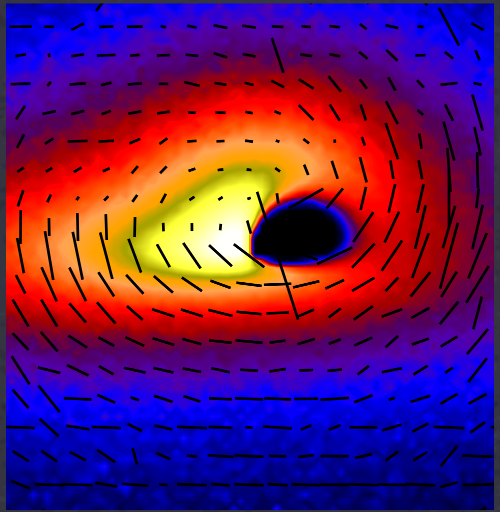

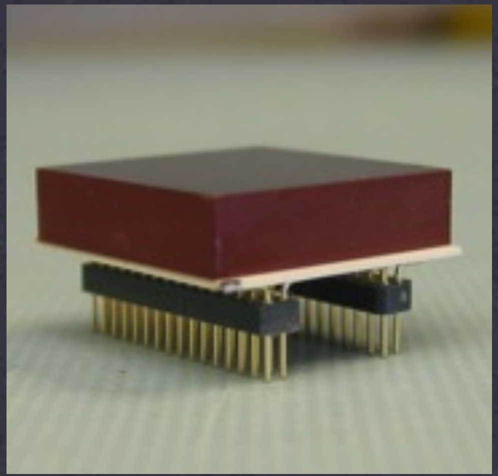

Plan of Talk:

- Motivation: X-Ray Polarimetry.
- CZT Detectors:
  - Development.
  - Exemplary architectures.
- Summary.

X-Ray Observations

Chandra & XMM Newton
(1999-present, 0.1-12 keV)

Tycho Super Nova Remnant

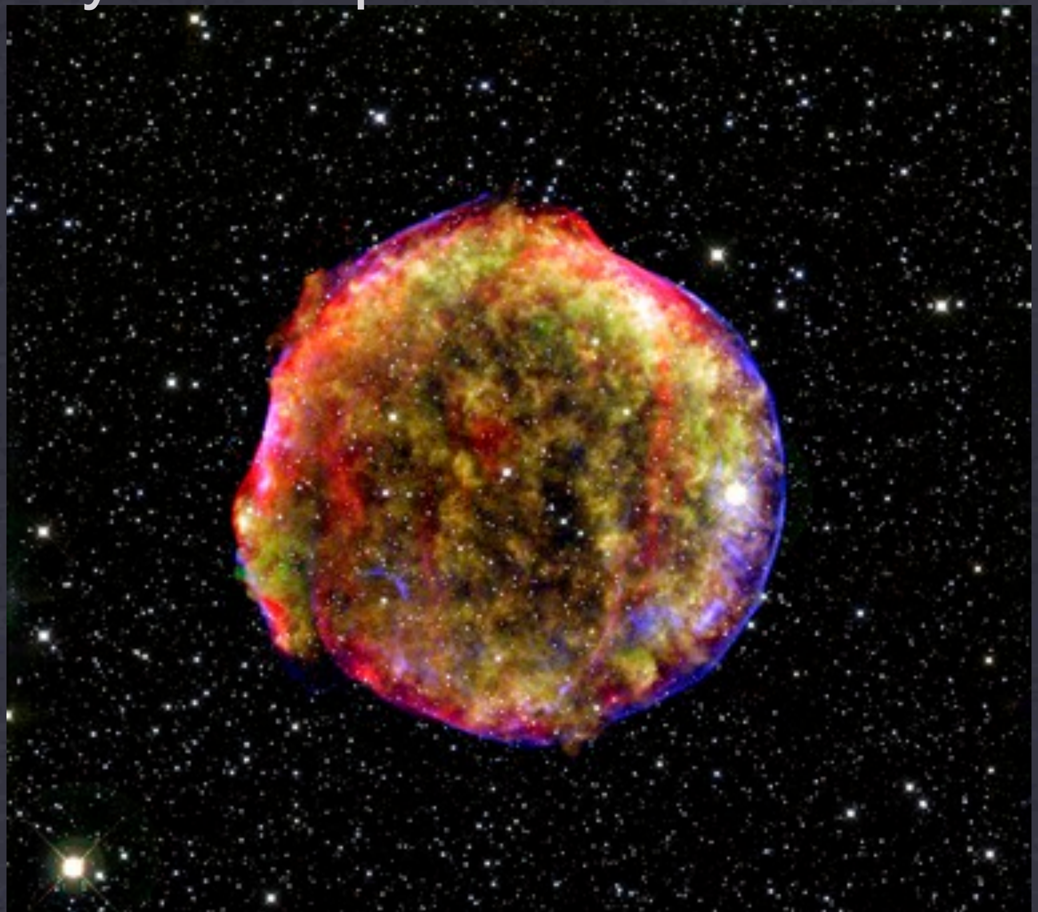

Imaging spectropolarimetric data

⟹ Riccardo Giacconi receives Nobel Price in Physics for X-ray Astrophysics (2002).

- ***Few polarimetric results***, except Crab Nebula, Cyg X-1 with OSO-8 (Weisskopf et al. 1978) and Integral (Dean et al. 2008, Laurent et al. 2011).

- Polarization measurements:

  ⟹ **Statistics**

  (5% pol. degree: ~10,000 γ's for 99% confidence level detection)

  ⟹ **Systematics**

  (~10% systematic errors on Integral results)

X-Ray Polarimetry

GEMS Gravity and Extreme Magnetism SMEX (2-10 keV)

Swank et al., GSFC

X-Calibur (5-70 keV, 20-70 keV):

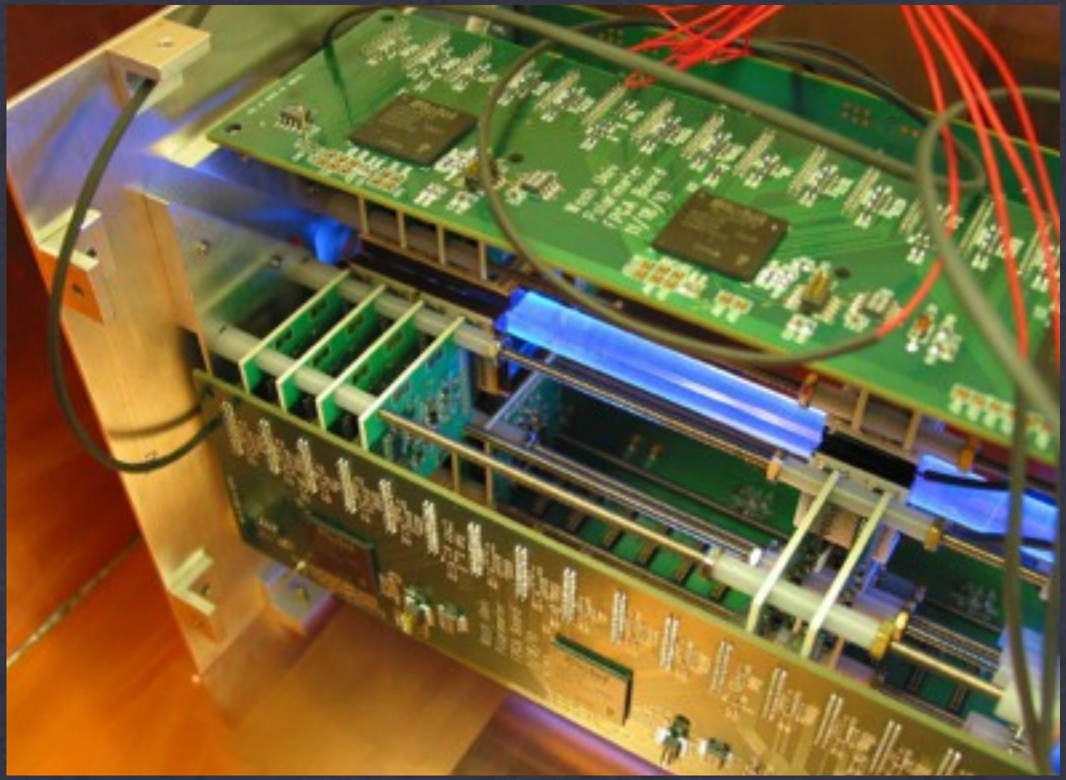

Krawczynski, Beilicke, Guo, Kislat et al.

Photoelectric effect polarimeters:

- 4 Time Projection Chambers, each 30 cm demethyl ether at 0.25 atm.

Compton effect polarimeter:

- 14cm scintillator rod surrounded by 32 CZT detectors.

Hard X-Ray Polarimetry with X-Calibur

- 1.6 ton payload,
- 40 km flight altitude,
- Pointing accuracy: 0.015°

- 255 shell Al mirror;
- 50 cm^2 area at 30 keV;
- (Pt/C coating).

Hard X-Ray Polarimetry with X-Calibur

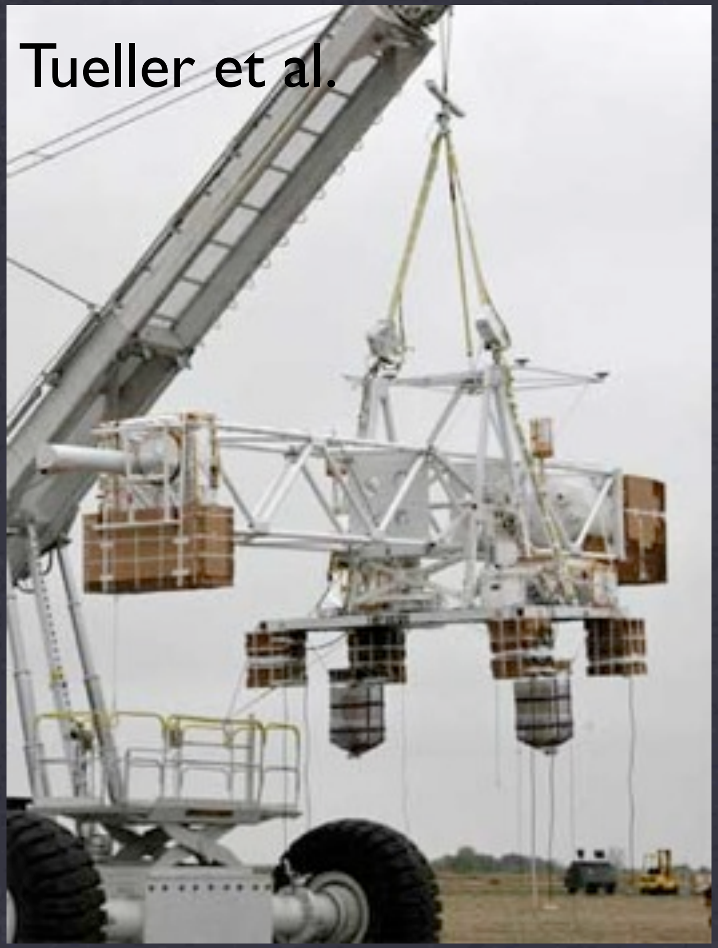

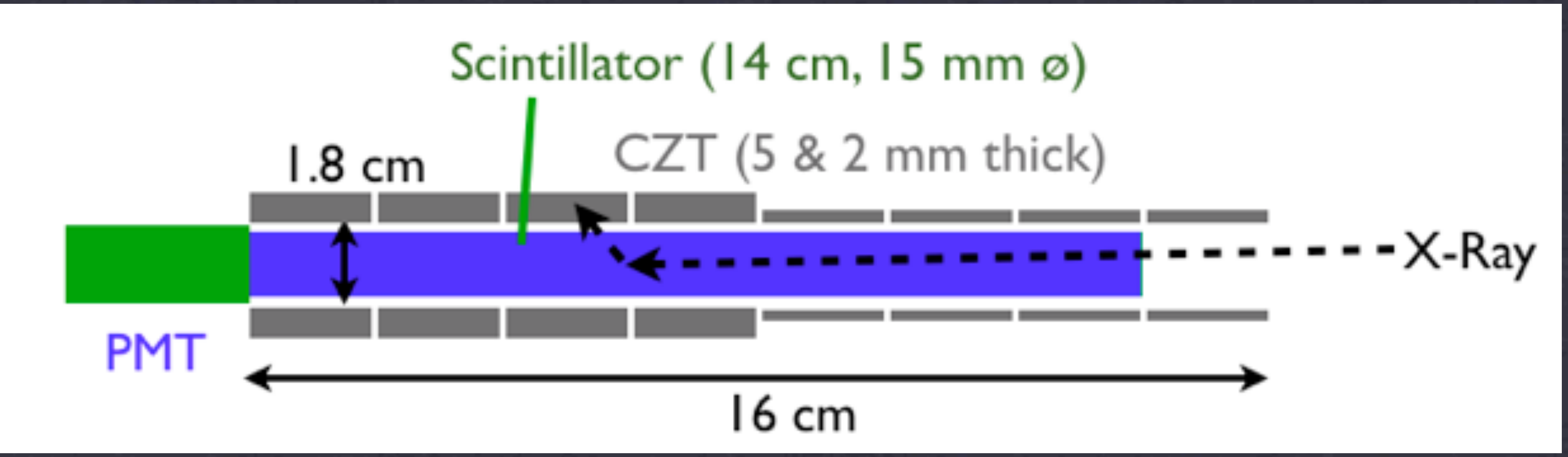

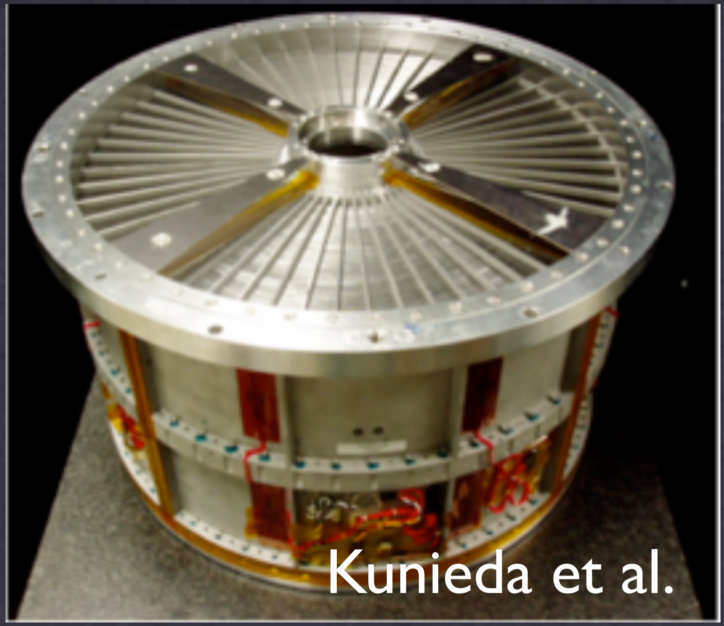

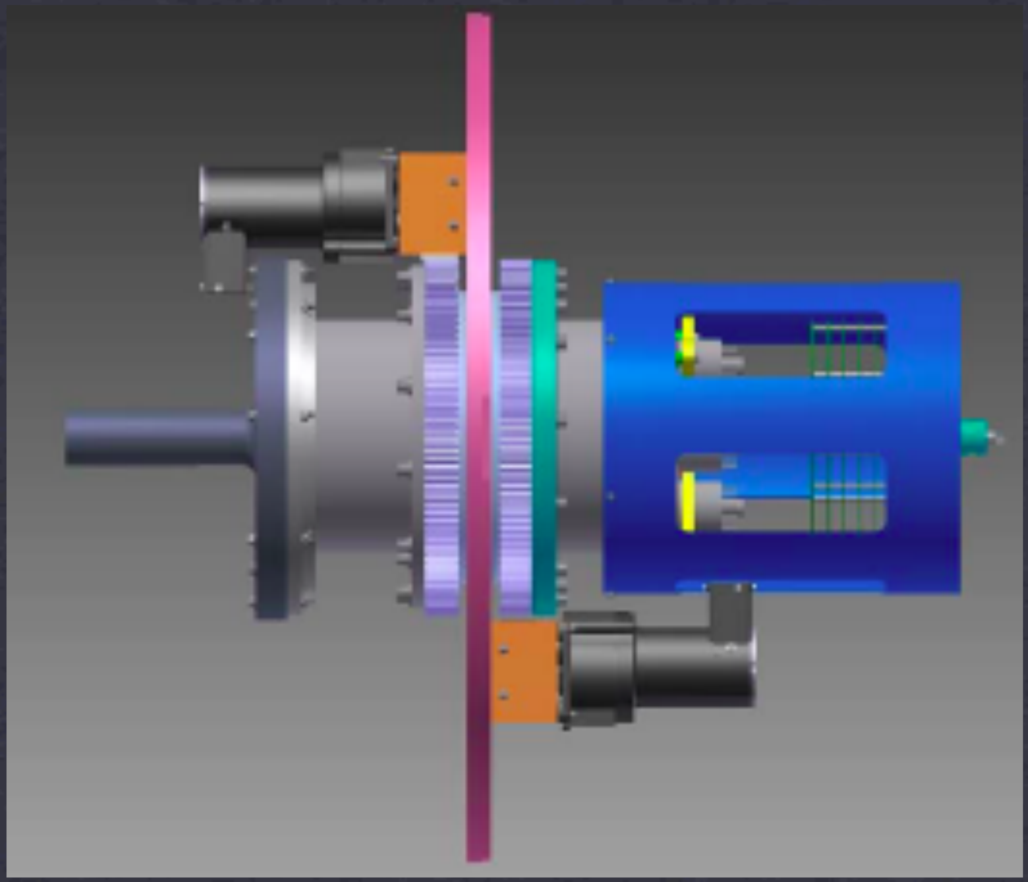

Rotation: cancel systematics.

Results with Polarized Beam

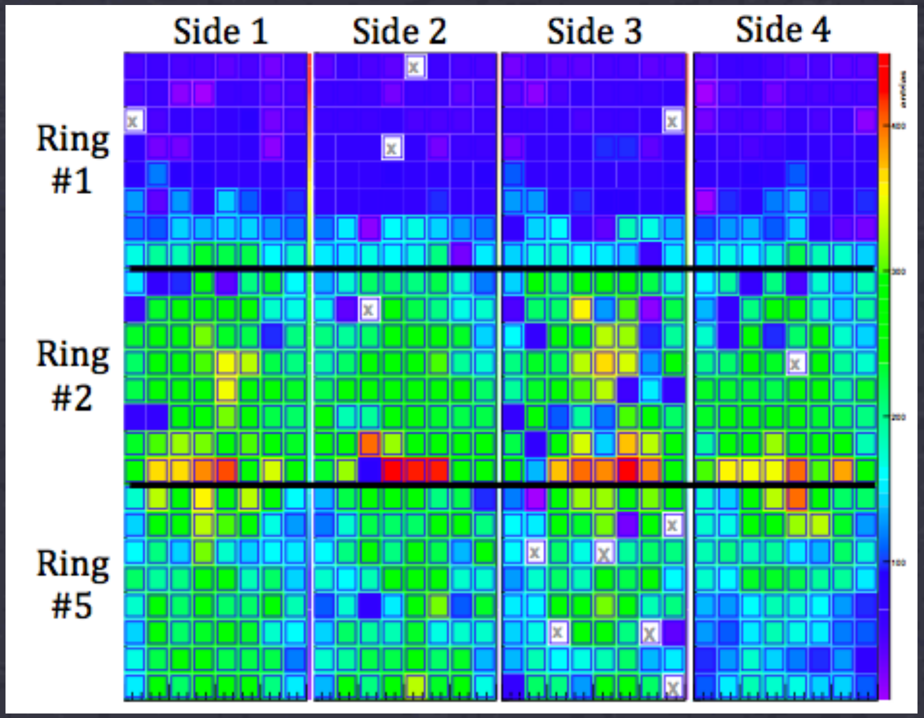

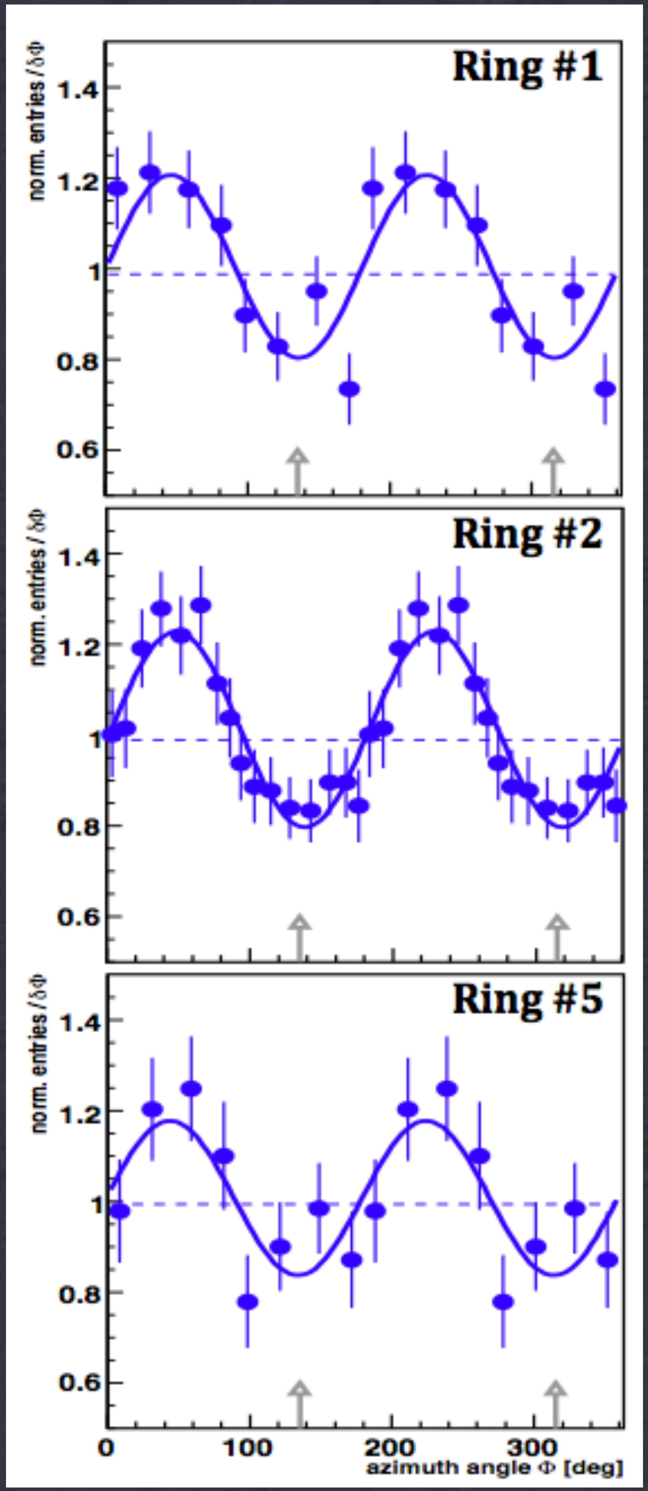

Reconstructed polarization fraction: 52%.

One-Day Balloon Flight (Fort Sumner, NM, 2013): Observe Cyg X-1, GRS 1915, Crab, Her X-1, Mrk 421 with 4% MDP for Crab.

Science Driver: X-ray Polarimetric Observations of Black Holes

Cygnus X-1:

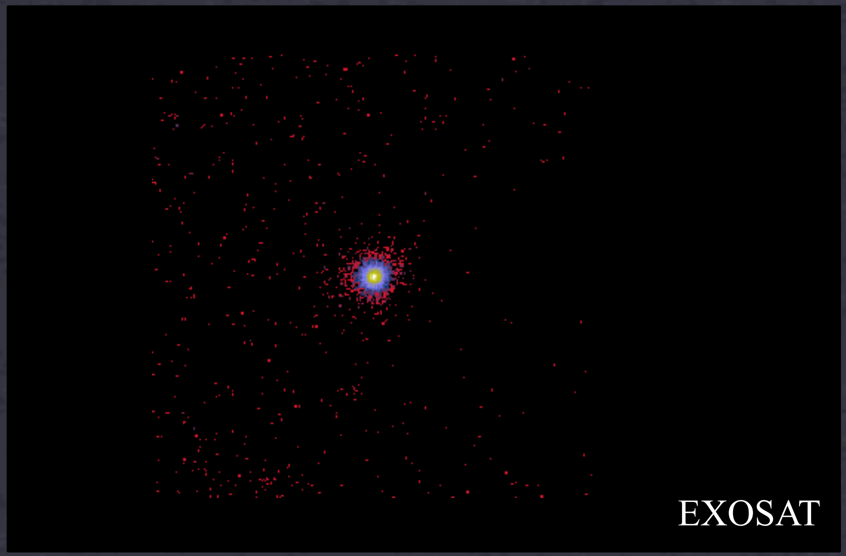

19 $M_\odot$ O-star orbits "invisible" 15 $M_\odot$ companion with 5.6 day period.

Stellar mass black hole in X-ray binary:

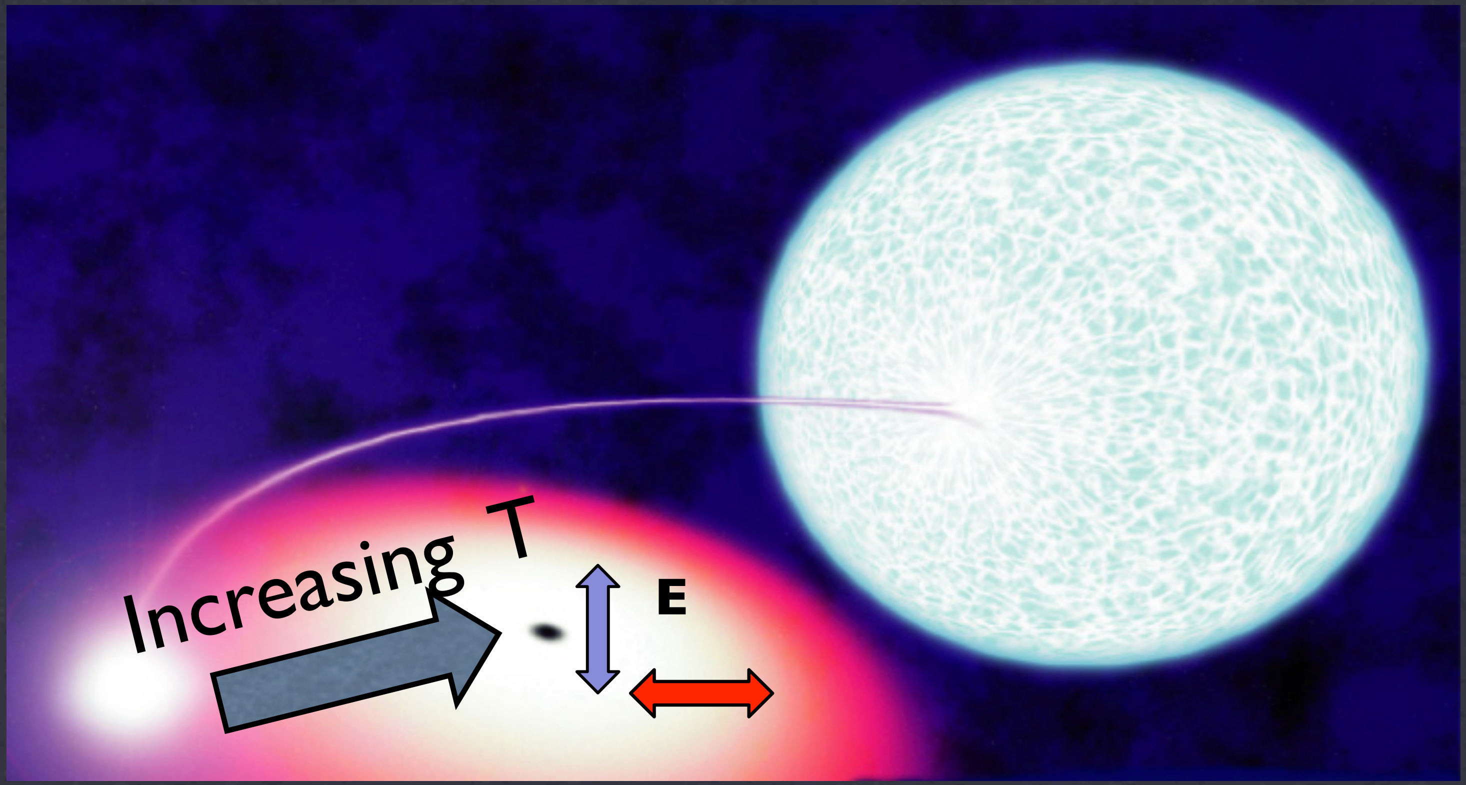

• Energy resolved (non-imaging) polarimetry $\Longrightarrow$ map accretion flow and spacetime!

Science Driver: X-ray Polarimetric Observations of Black Holes

Guo et al. (2011):

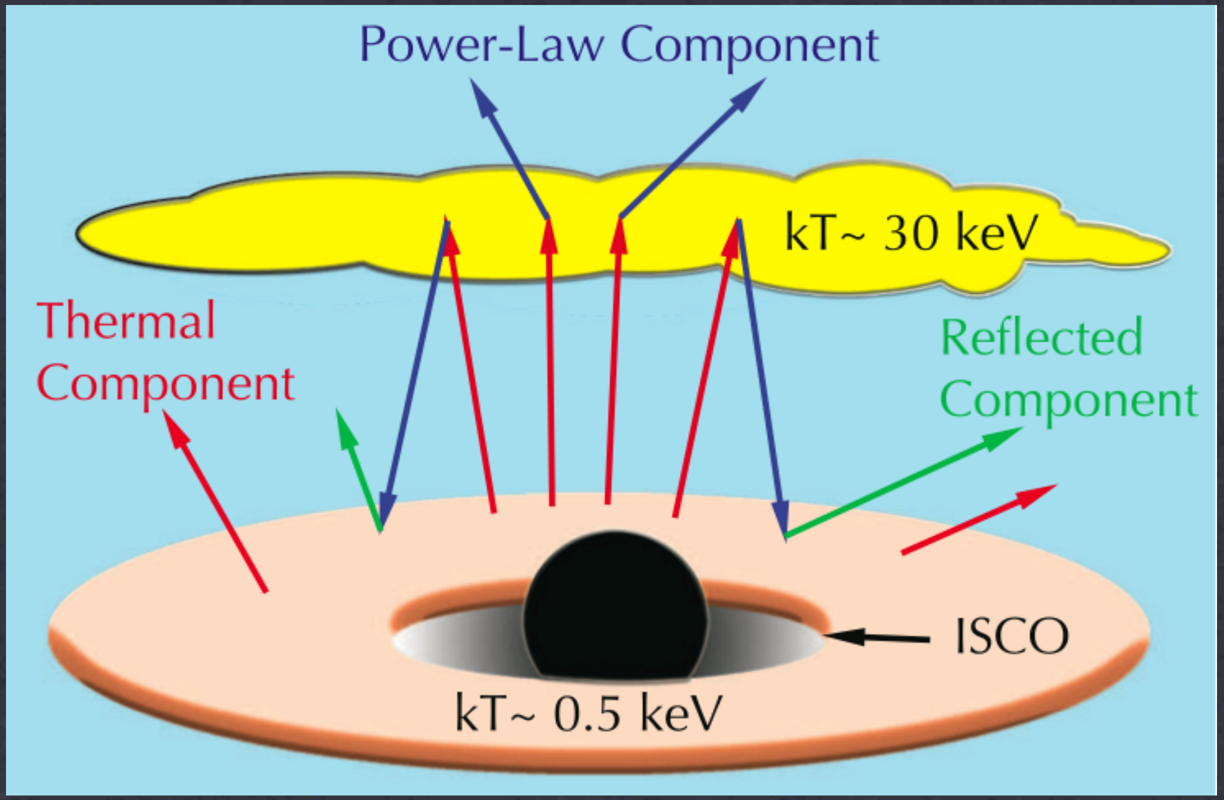

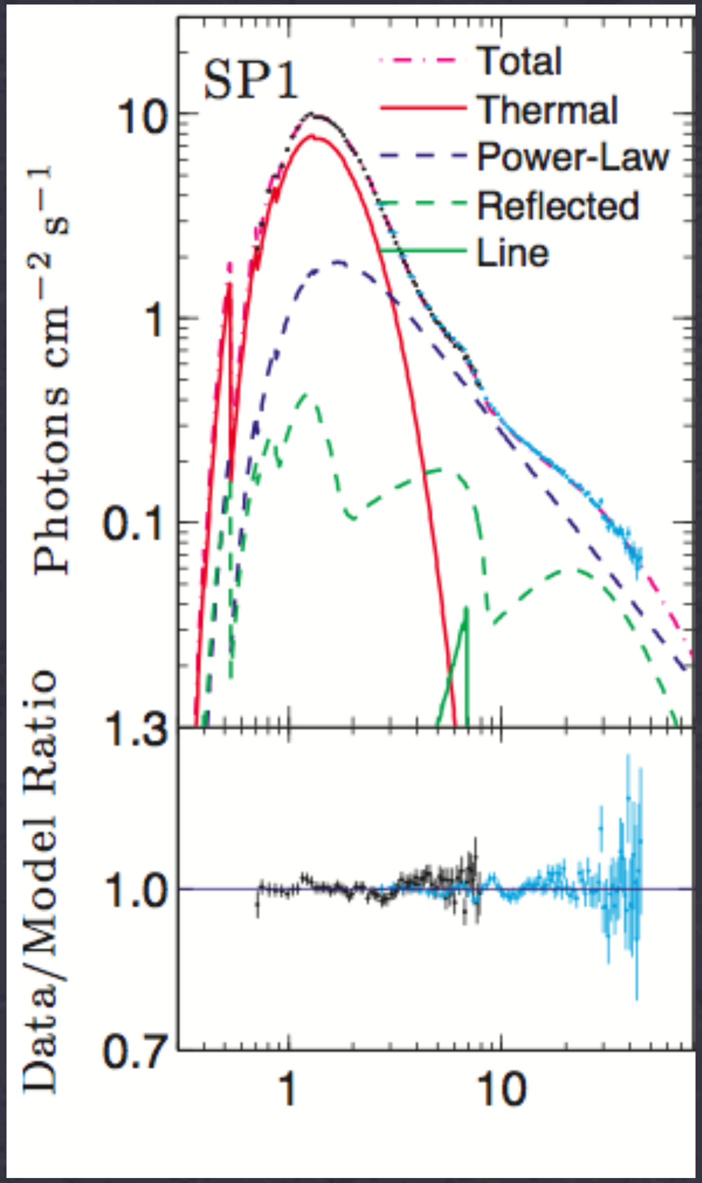

$$a_* = \frac{cJ}{GM^2} > 0.97\,(3\sigma)$$

X-ray polarimetry (0.5-100 keV):

- Test Accretion Disk Models.
- Test No-Hair Theorem of GR.
- Constrain corona geometry.

Simulation Results

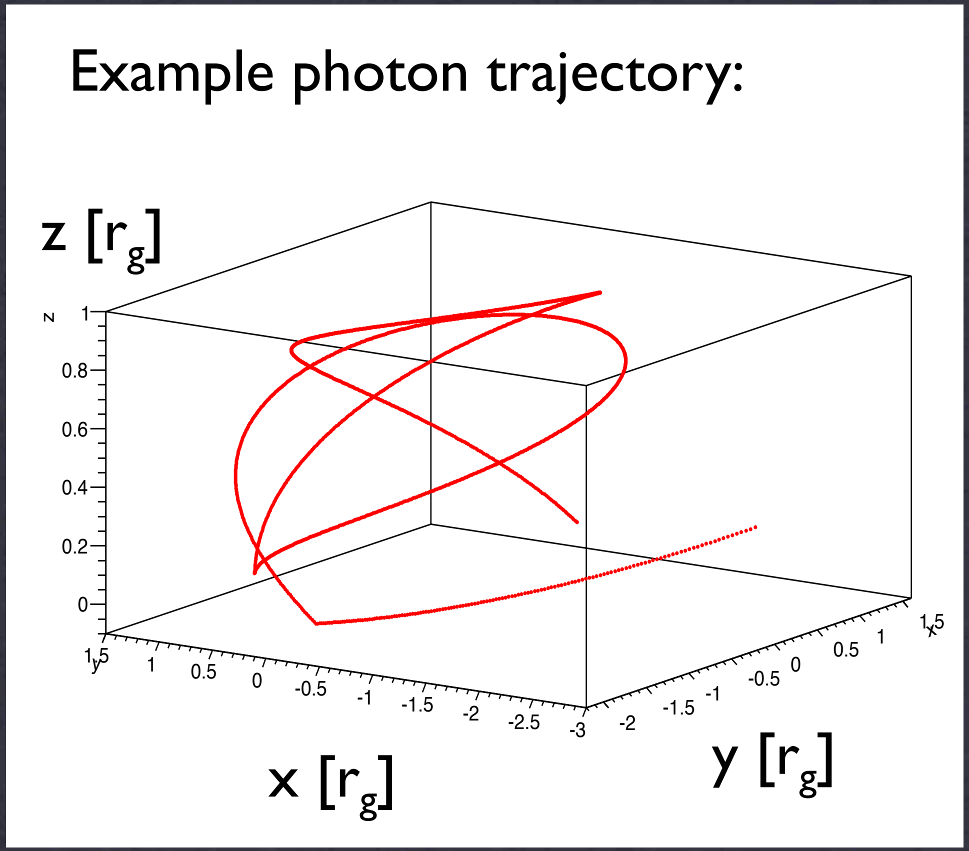

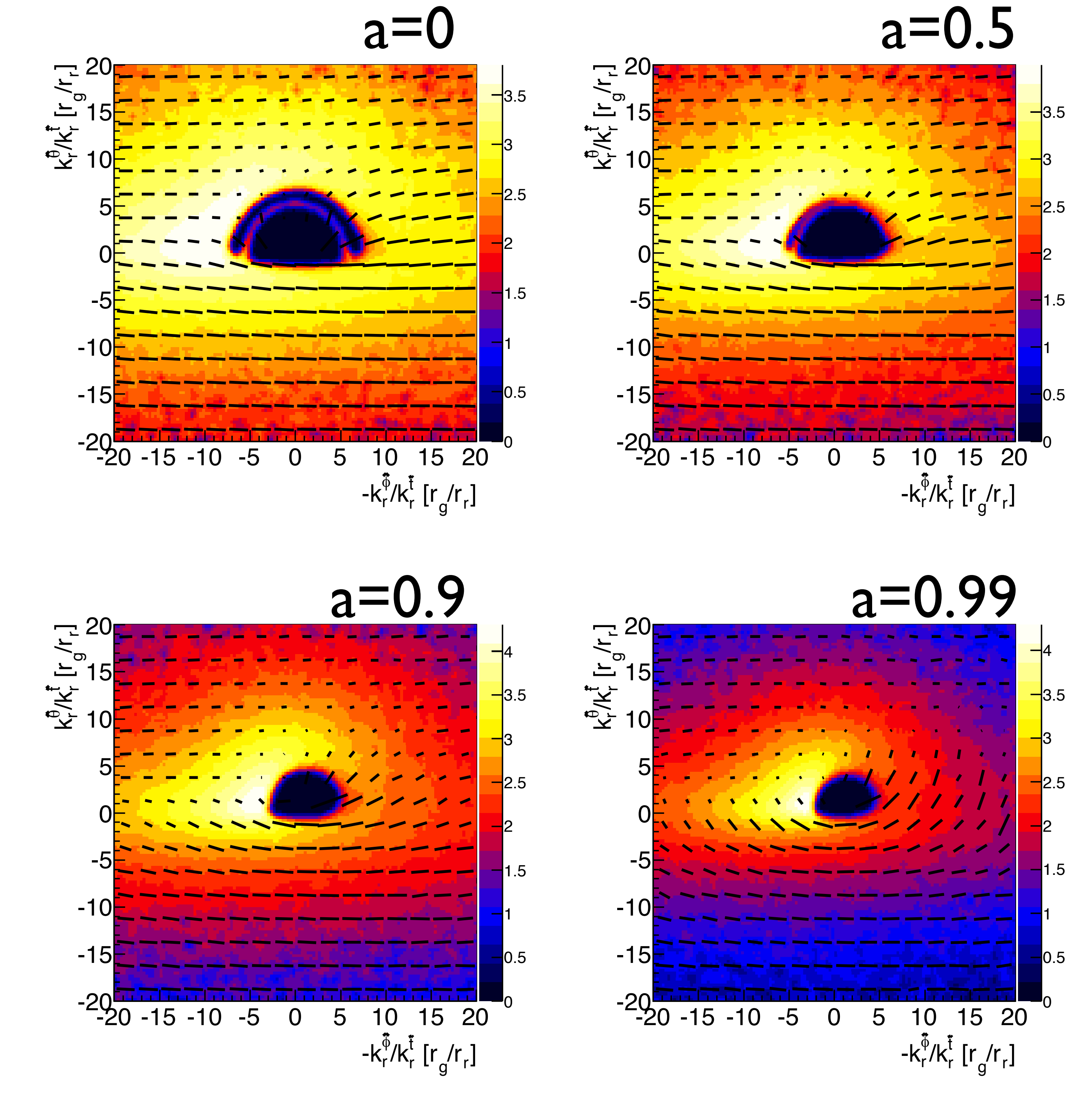

$M = 10\ M_{sun}$
$L_{Disk} = 0.1\ L_{edd}$
$i=75^{\circ}$

HK (2012, ApJ, in press, arXiv:1205.7063)

Simulation Results

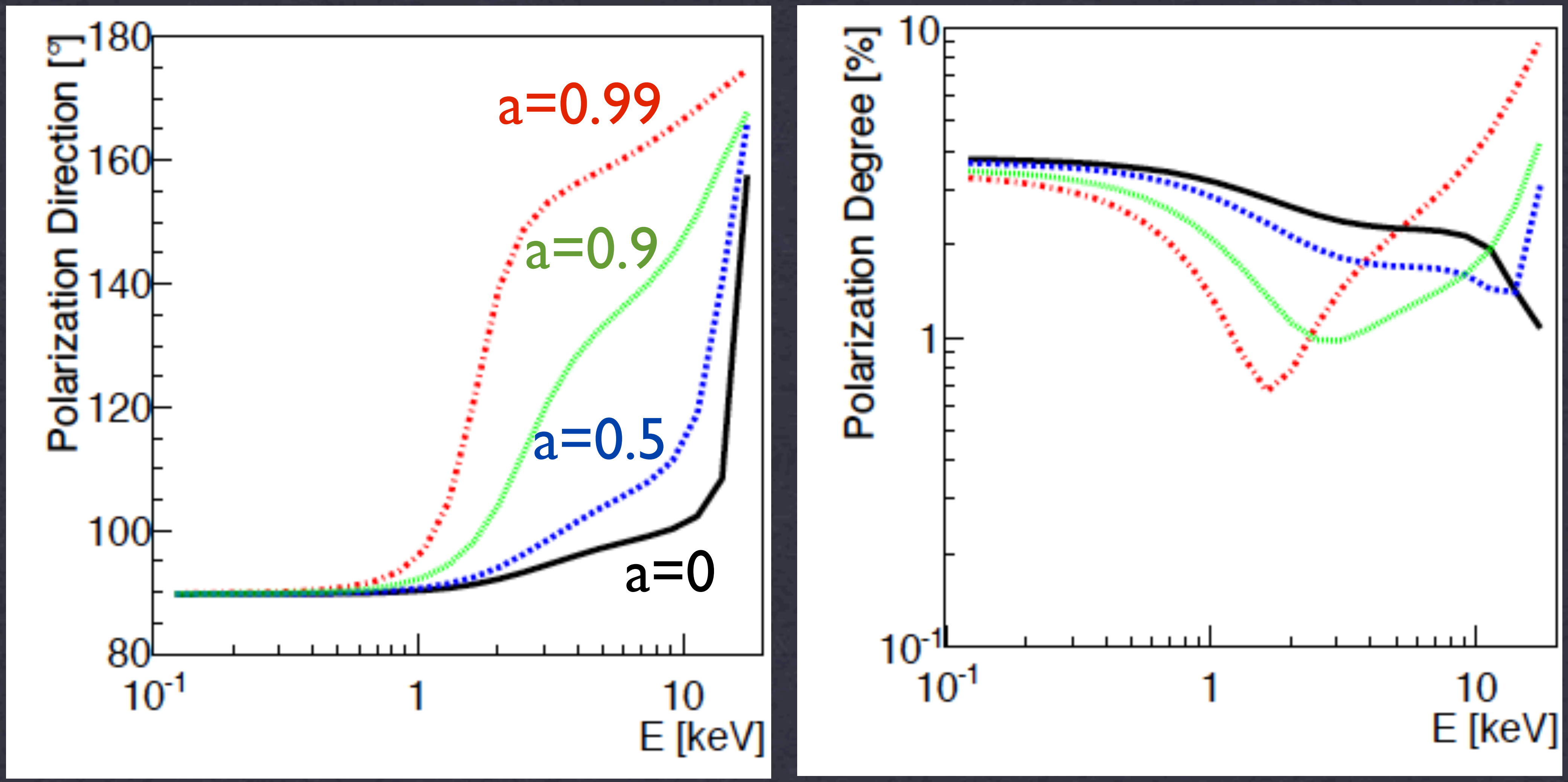

⟹ Measure Black Hole Spin and some (but rather limited) sensitivity to test No Hair Theorem (HK 2012).

Also: Connors et al. (1980), Schnittman & Krolik (2010).

Cadmium Zinc Telluride X-Ray and Gamma-Ray Detectors

- $Cd_{(1-x)}Zn_xTe$; x~0.1.
- Large direct band-gap:
  - E_g = 1.57 eV; E_i = 4.64 eV
  - Room-temp operation!
- High stopping power:
  - High <Z>: 49.1,
  - High-density: 5.78 g cm
  - Detector thickness: 0.2...1.5 cm.
- Detector Units (Endicott, Orbotech, Redlen, Creative Electron, Qickpak):
  - Standard: 0.5x2x2 cm^3;
  - Large: 0.5x4x4 cm^3 & 1.5x2x2 cm^3.
- Electronic properties:
  - $\mu\tau|_e = 5 \times 10^{-3}$ cm^2 V^{-1};
  - $\mu\tau|_h = 5 \times 10^{-5}$ cm^2 V^{-1}.

Pixel Detector

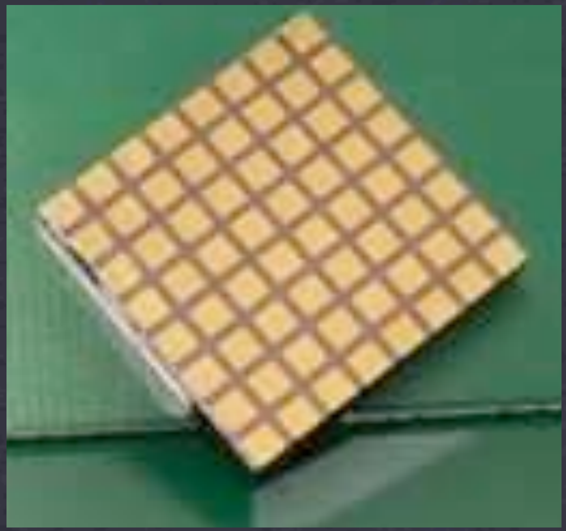

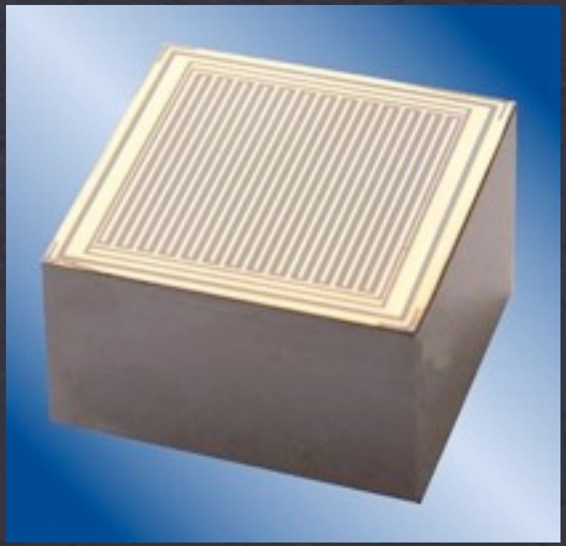

Coplanar Grid Detector

Planar Detectors vs. Small Pixel Detectors

Si, Ge Detectors

Planar CZT Detector

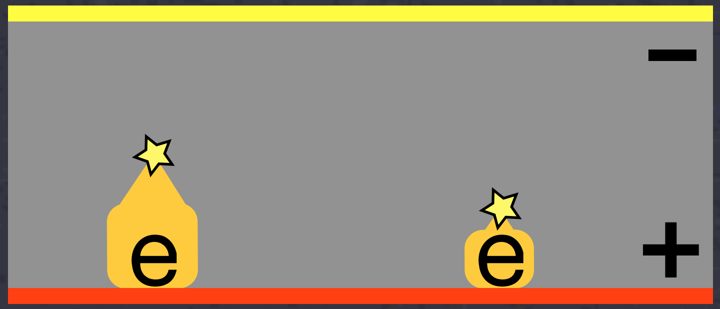

Pixel CZT Detector

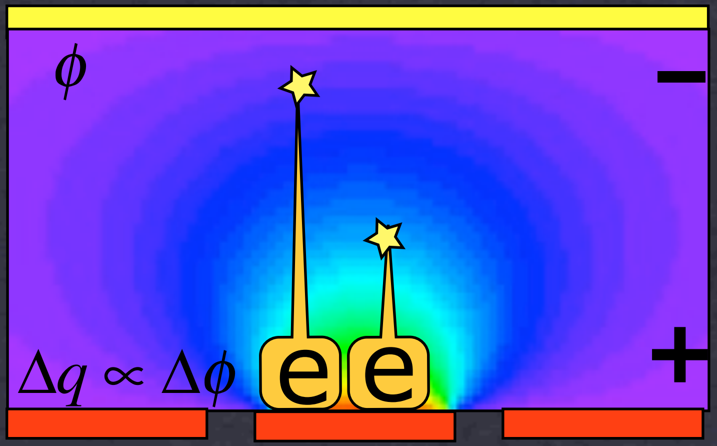

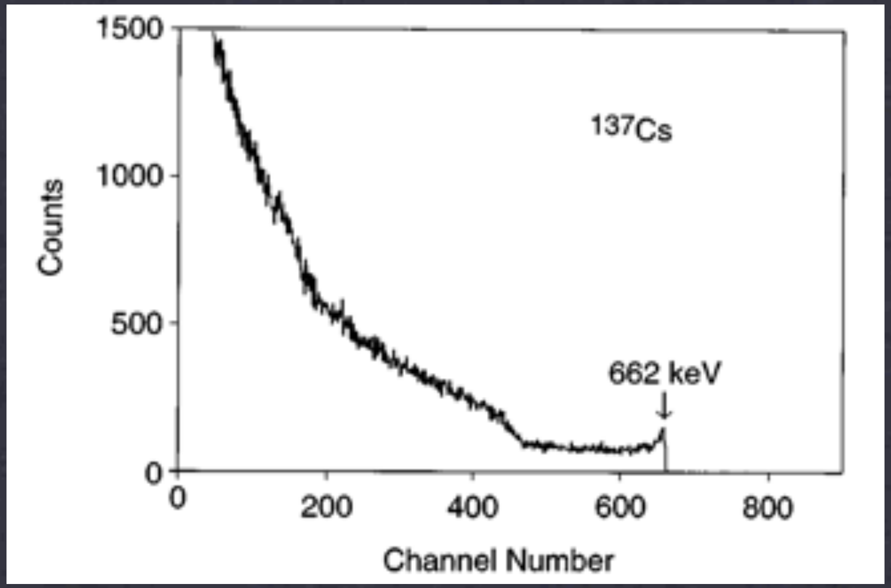

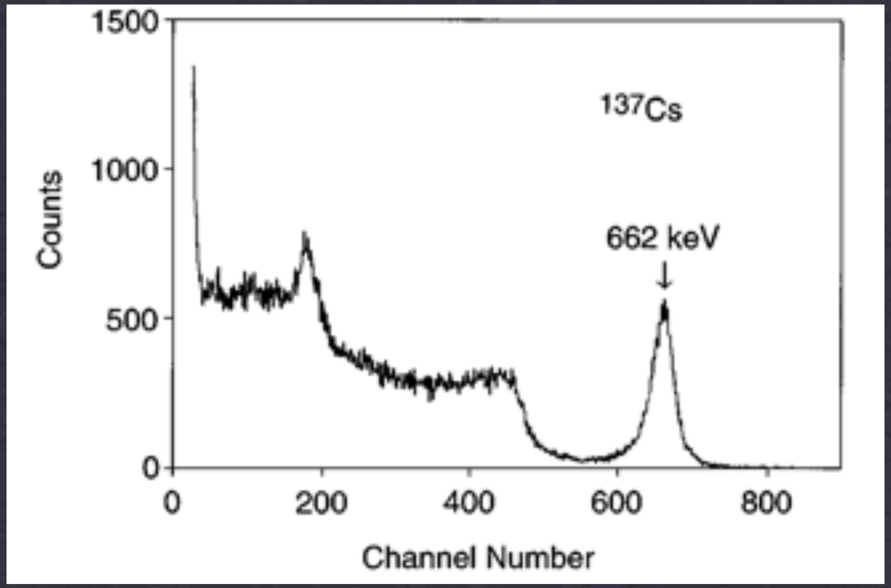

Barret et al., Luke et al. 1995

Applications for CZT Detectors

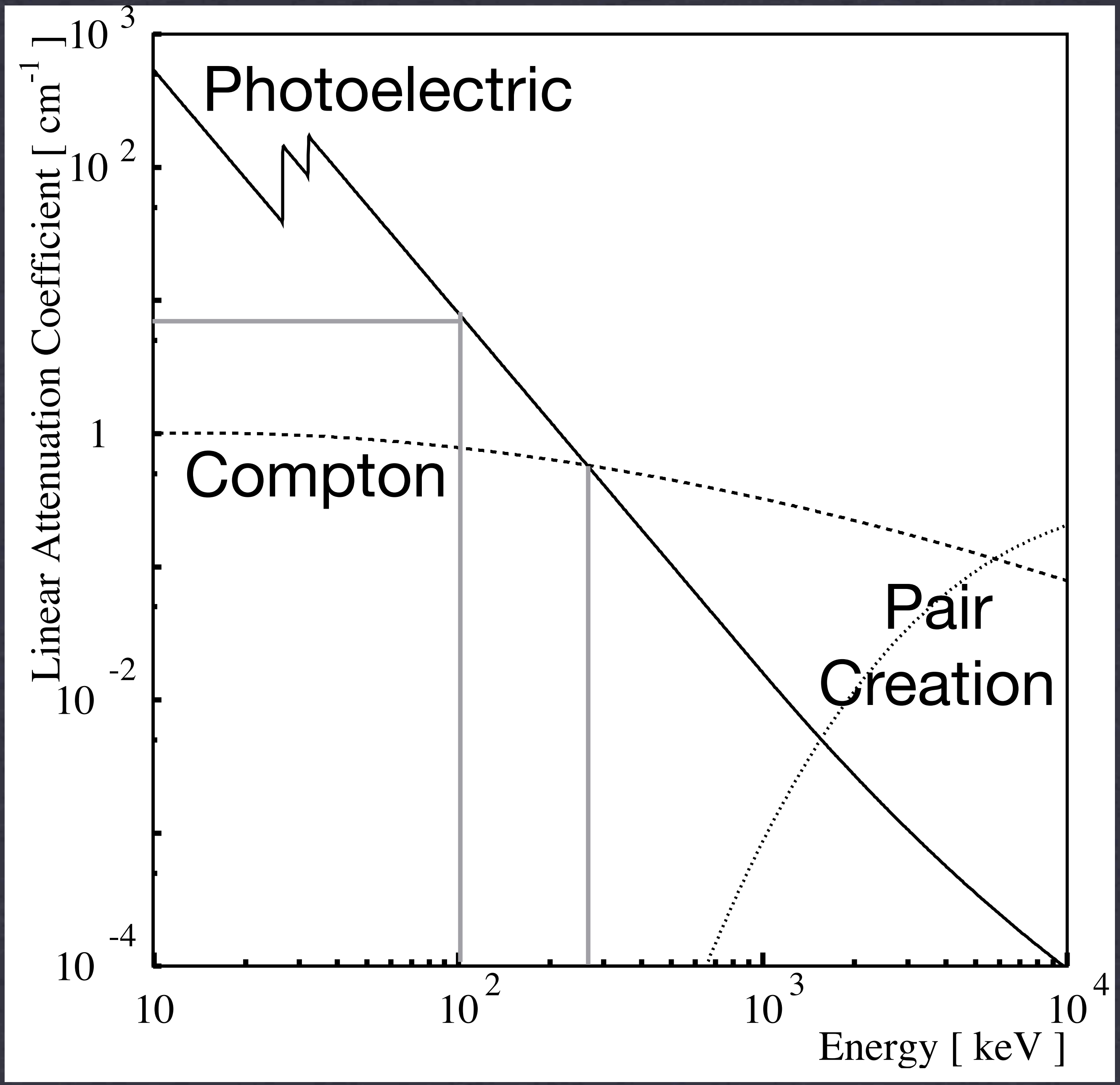

2-100 keV X-rays (vs. Si):
- Energy thresholds ≥2 keV.
- Energy res. 0.5-2 keV FWHM.
- Spatial resolutions ~ 1mm.
- Better stopping than Si.
- Higher σ_{PE}/σ_{C}.

>100 keV gamma-rays
(vs. Scint. & Germanium):
- Better energy (<1% FWHM @ 662 keV) and spatial resolutions than the best scintillators.
- No need for cryogenic cooling.

Material of choice for many spectroscopic photon detection in

Detector Fabrication:

- Polish with abrasive.
- 5% Br, 95% Methanol wet etch;
- Photolithography;
- Contact deposition with e-Beam evaporator.

Detector Fabrication

Optimization of Detector Contacts

Ti In

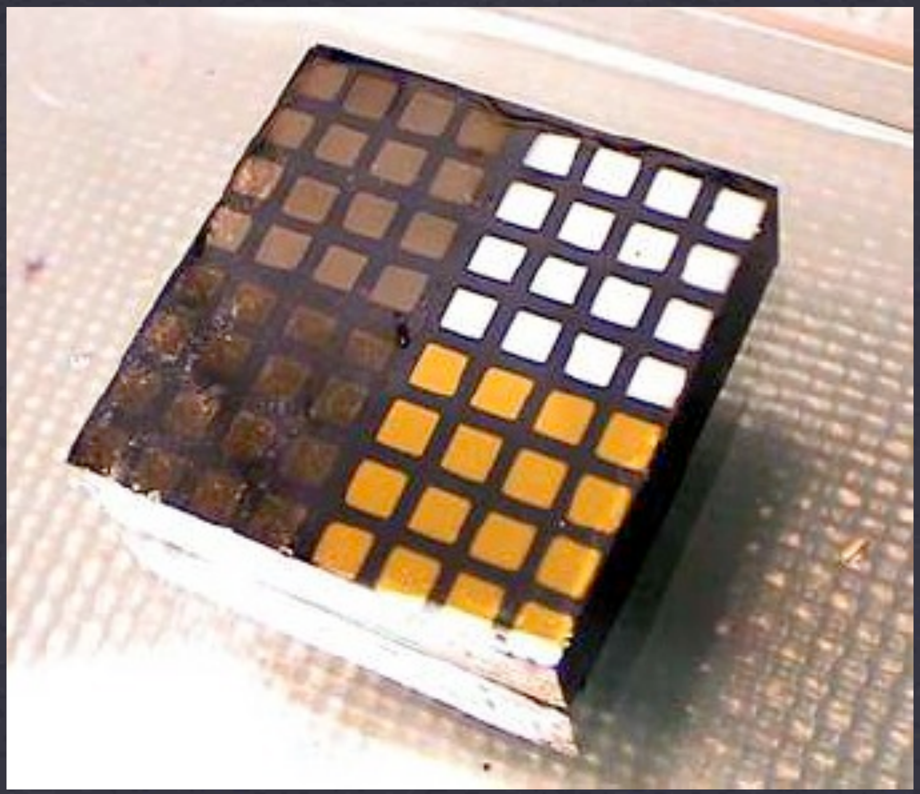

Cr Au

- Au on cathode:
  blocking contact on
  n-type CZT
  ⇒ reduced dark current.
- In & Ti on anode:
  ohmic contact on
  n-type CZT
  ⇒ reduced noise.

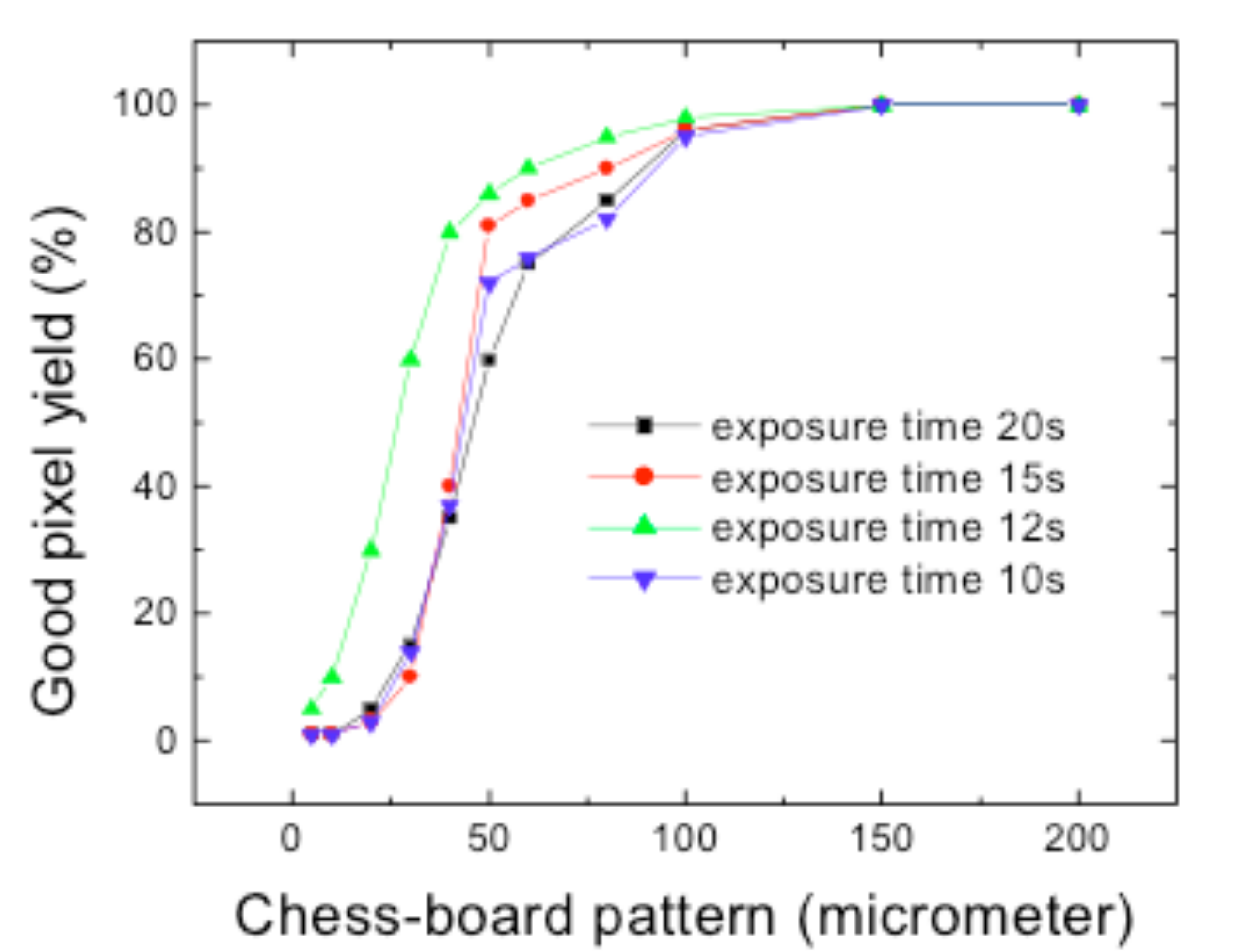

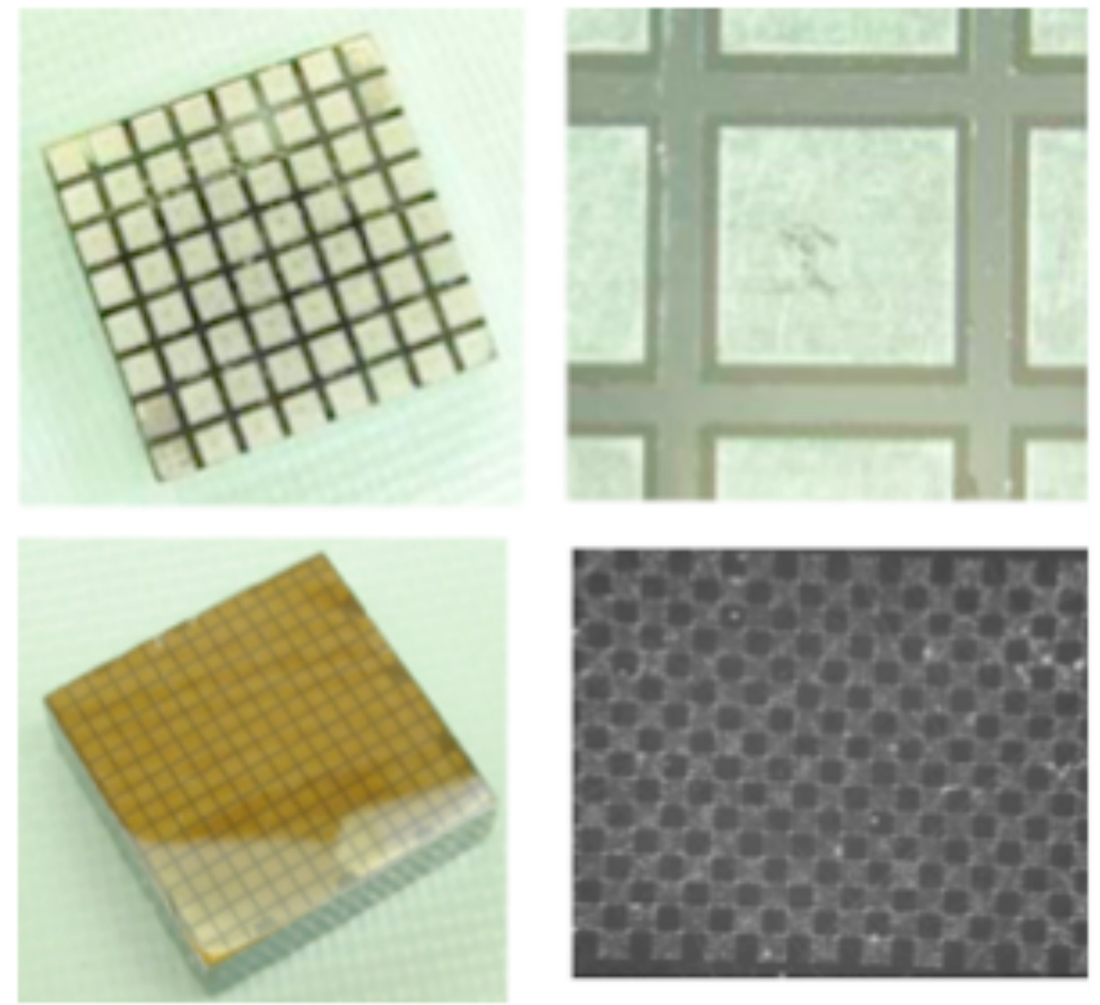

- Good yield for detectors with pixels at ~100 micron pixel pitch.

Optimization of Photolithography

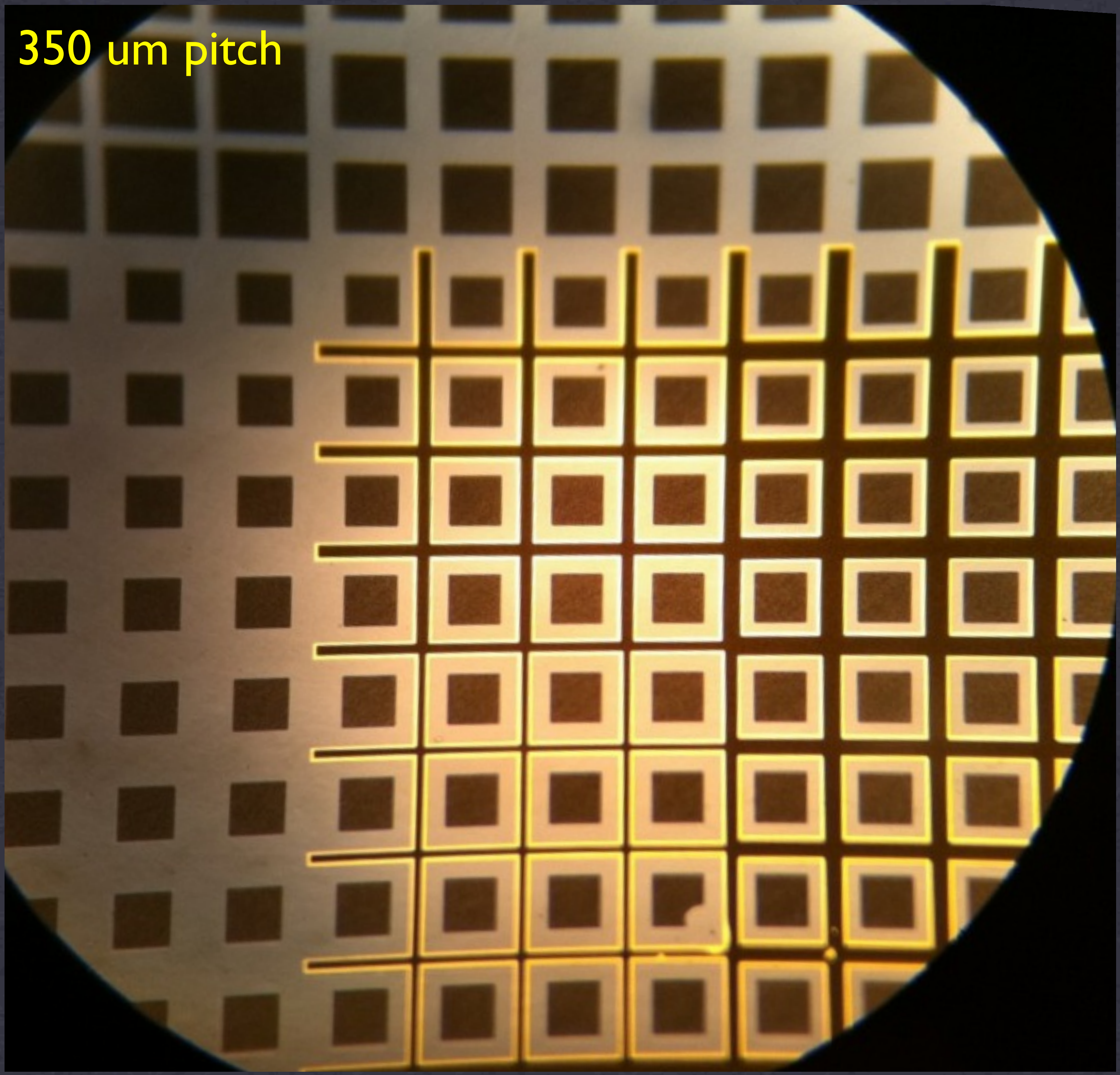

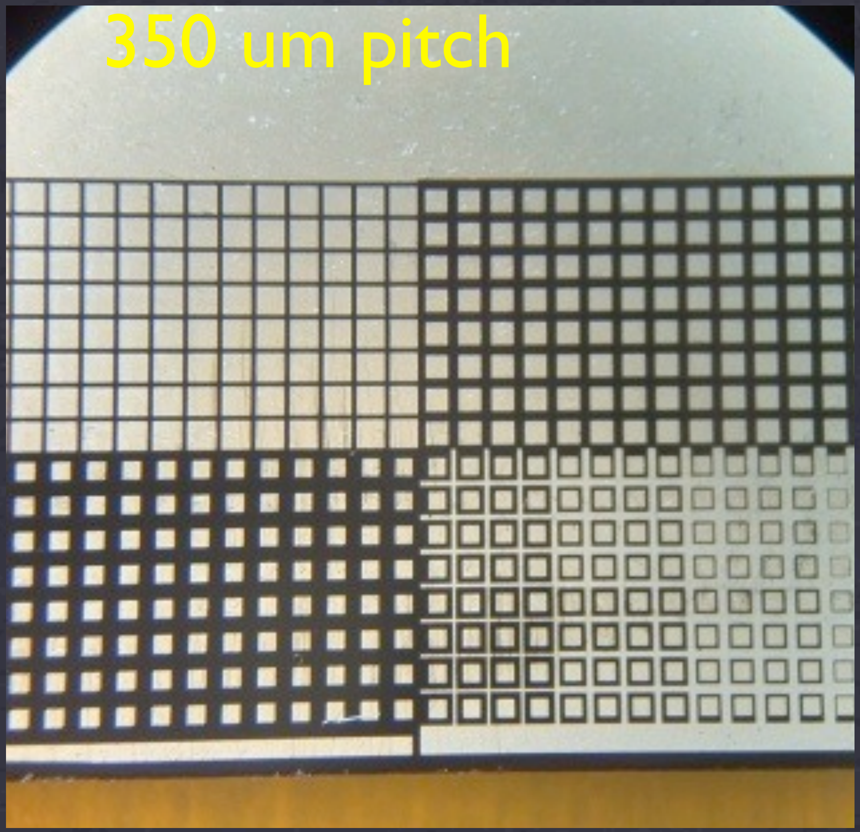

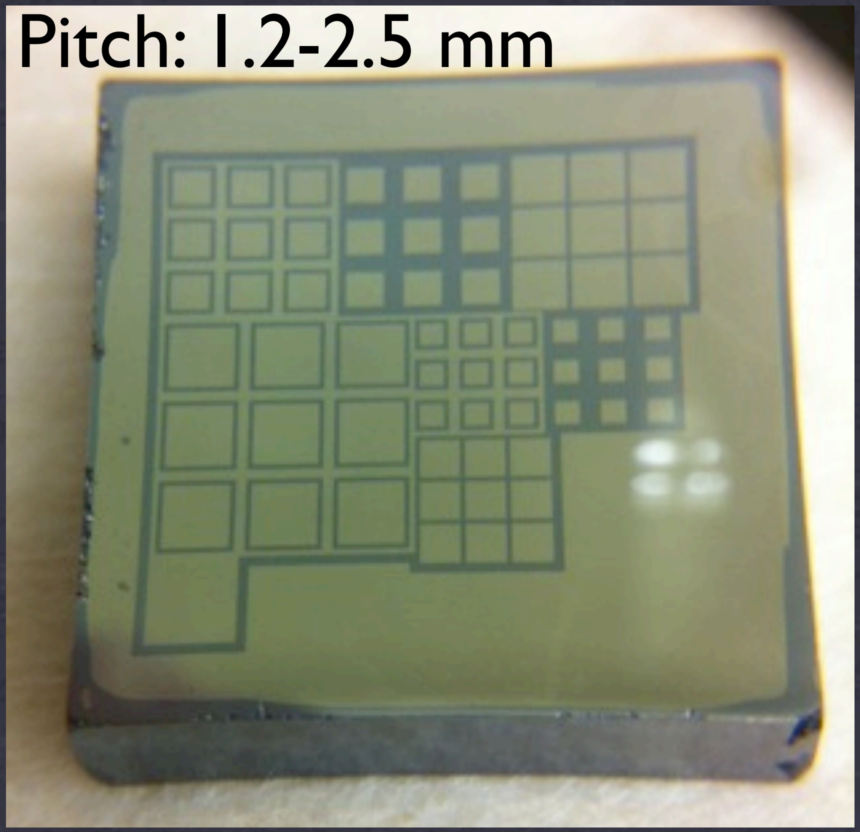

Pixelated Detectors

Alternative Contact Designs

Cross-strip CZT detector: 0.5 x 4 x 4 cm^3.

Dual-anode CZT detectors: 1 x 2 x 2 cm^3.

Limited energy resolutions (>~3%) and modest detection efficiency owing to modest small pixel effect and weak cathode signals.

Detector Systems

ASIC board:

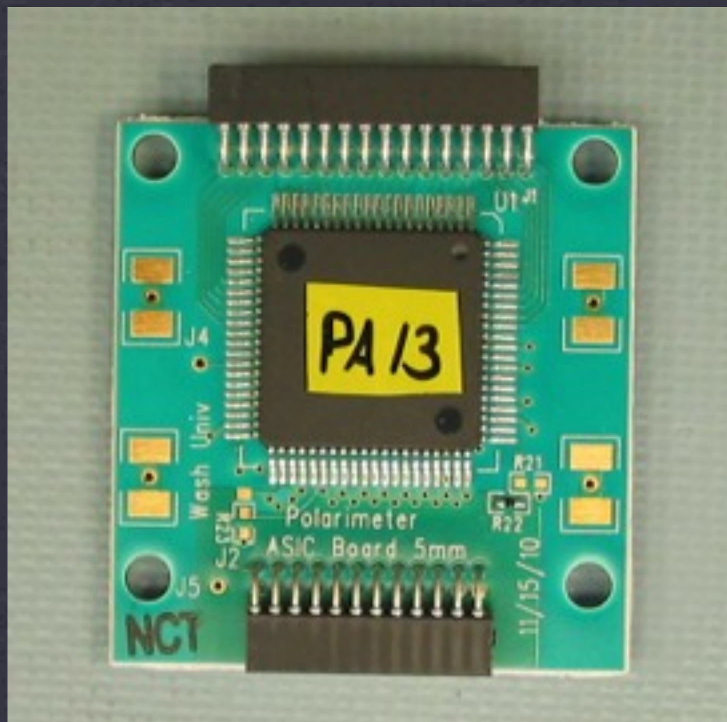

CZT on ceramic substrate:

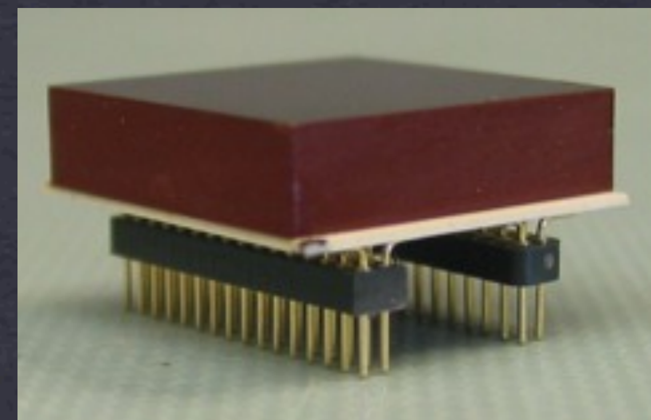

CZT on ceramic substrate:

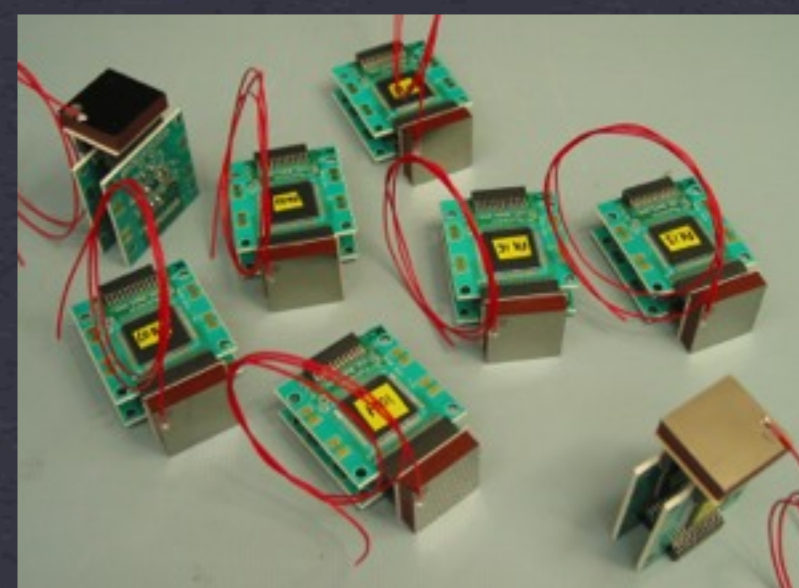

Tower with 8 detectors:

ASIC developed by G. de Geronimo (Brookhaven):
- 32 channel;
- 1-2 keV noise (FWHM).

Towards Smaller Pixels

- CZT with 4096 pixels at 350 μm pitch, footprint 2.24 x 2.24 cm^2;
- ASIC: 2048 channels ASIC (L. J. Meng, UIUC);
- Wash. Univ. readout system:

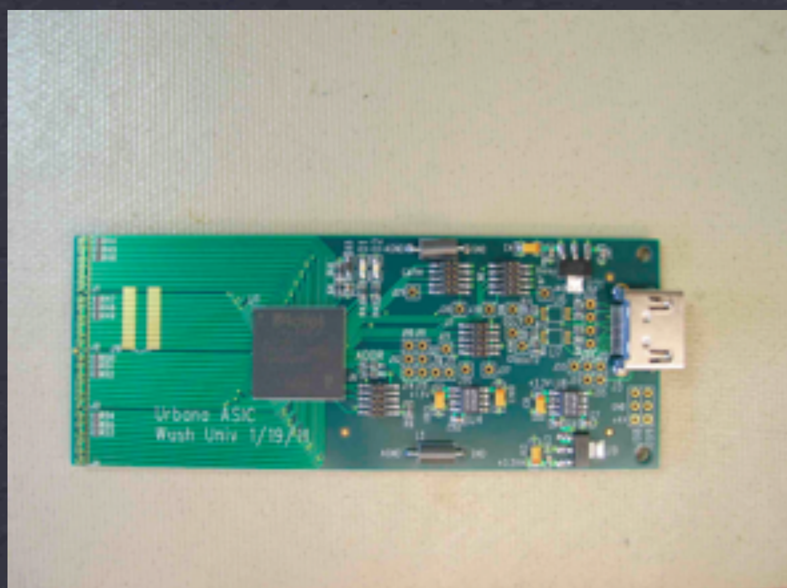

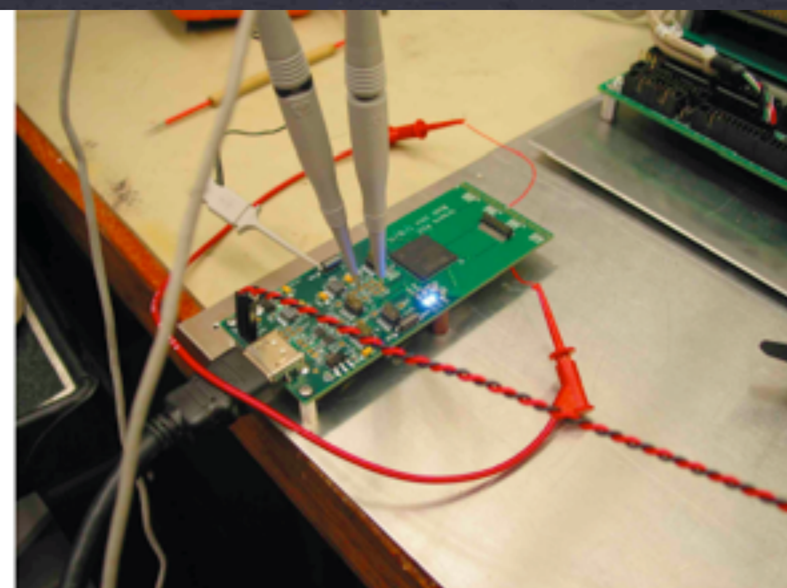

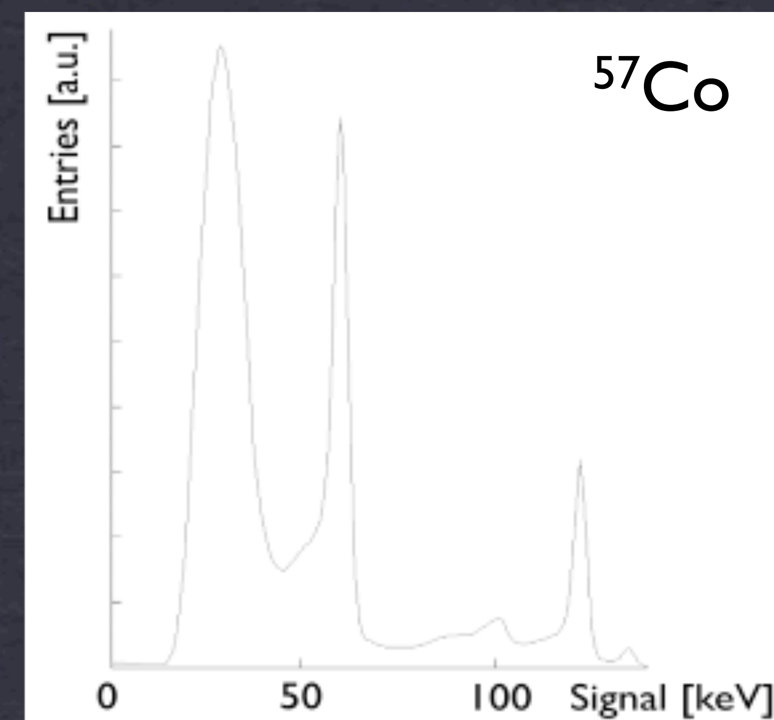

- CdTe detector (2mm).
- Energy res. 4 keV FWHM.

Infrared Imaging

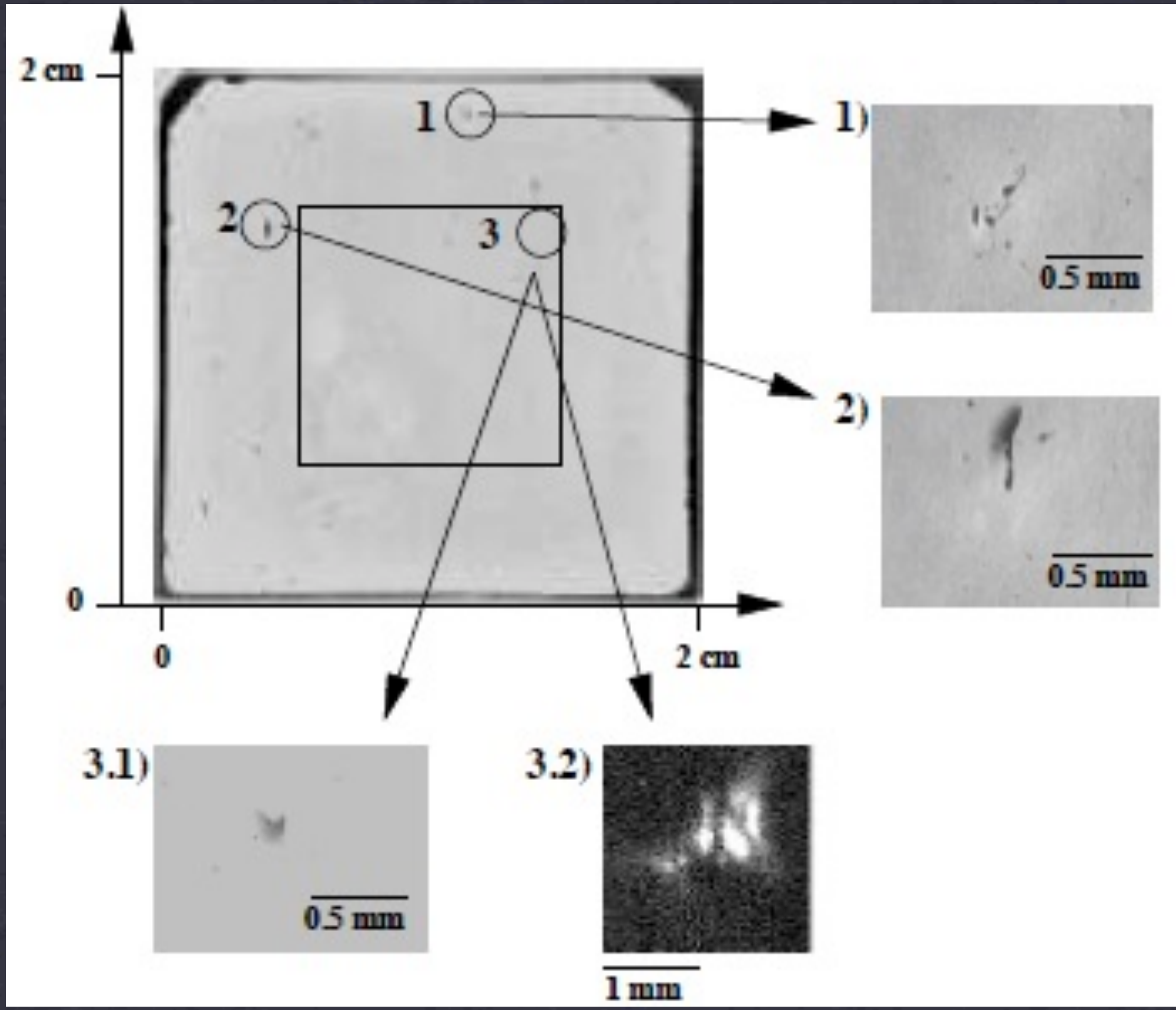

A. Burger, M. Groza
(Fisk University)
H. Krawczynski,
I. Jung (Wash. Univ)

- Infrared imaging (1.1 μm) reveals non-uniformities correlated with underperforming pixels.

Pockels Imaging

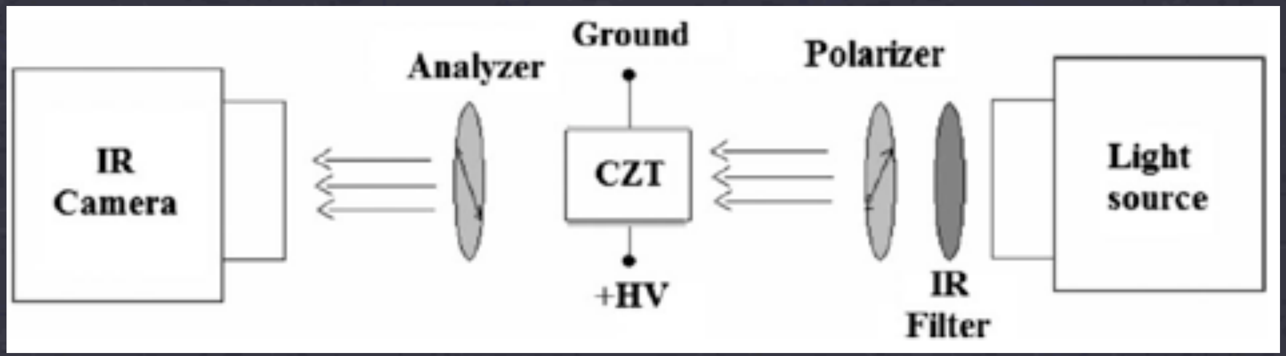

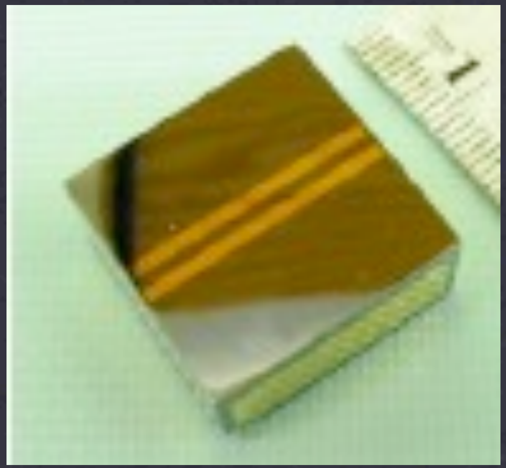

Pockels effect can be used to measure E-field.

E-field from Pockels
(CZT: 0.5x0.9x0.9 cm^3):

E-field from Simulations:

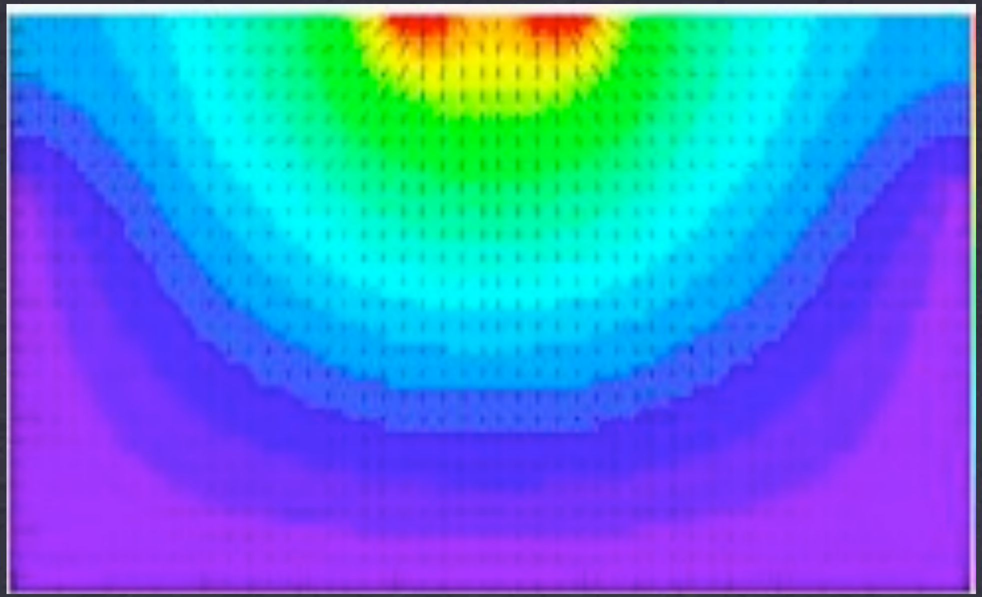

Groza et al. 2010

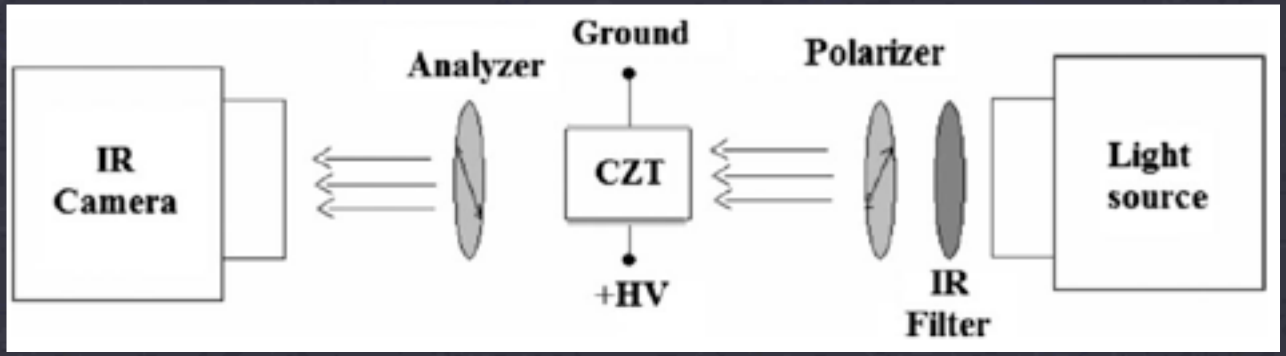

Pockels image of 0.5x1.9x1.7 cm^3 CZT detector suggests "layered E-field" inside detector.

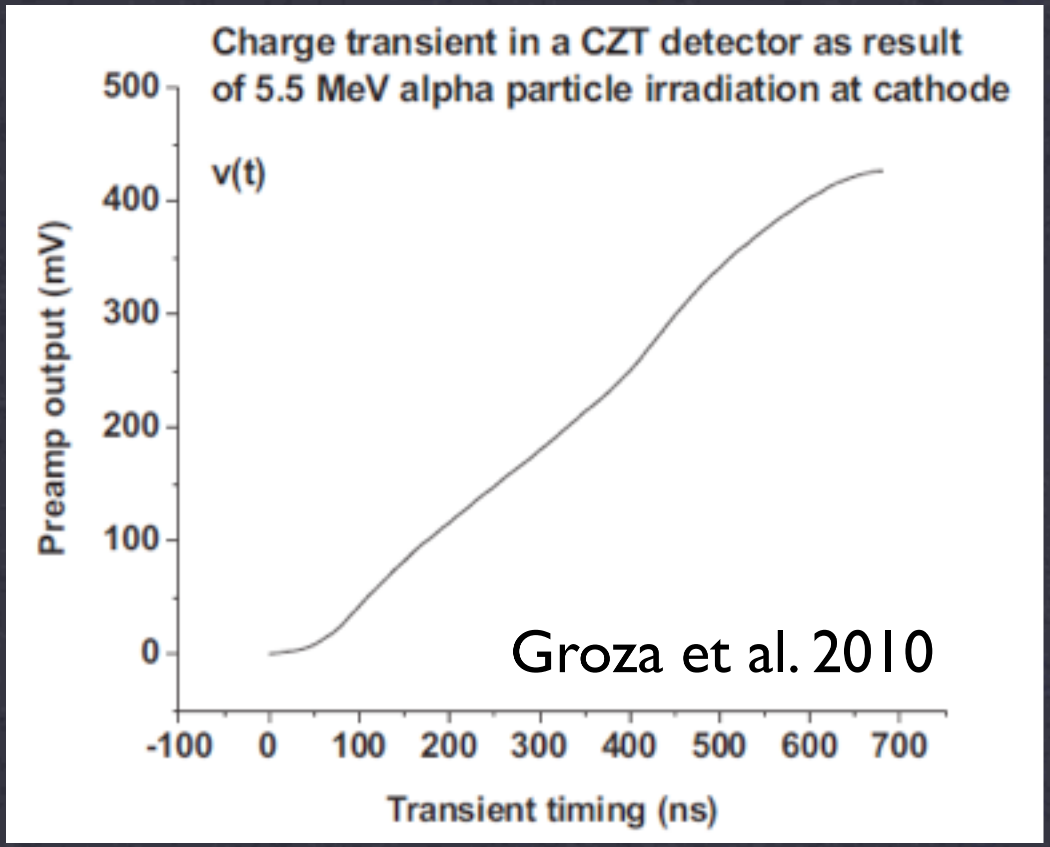

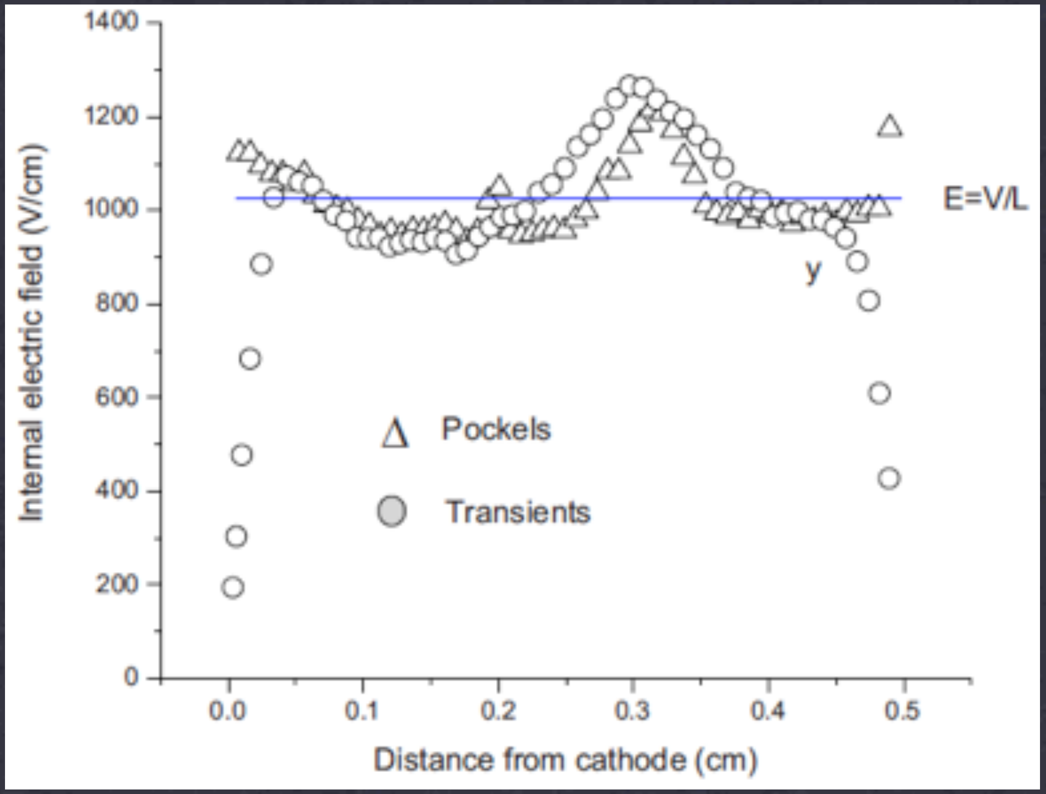

Transient analysis confirms results from Pockels imaging.

Pockels Imaging

Detector Simulations

Potential from 2-D Laplace solver:

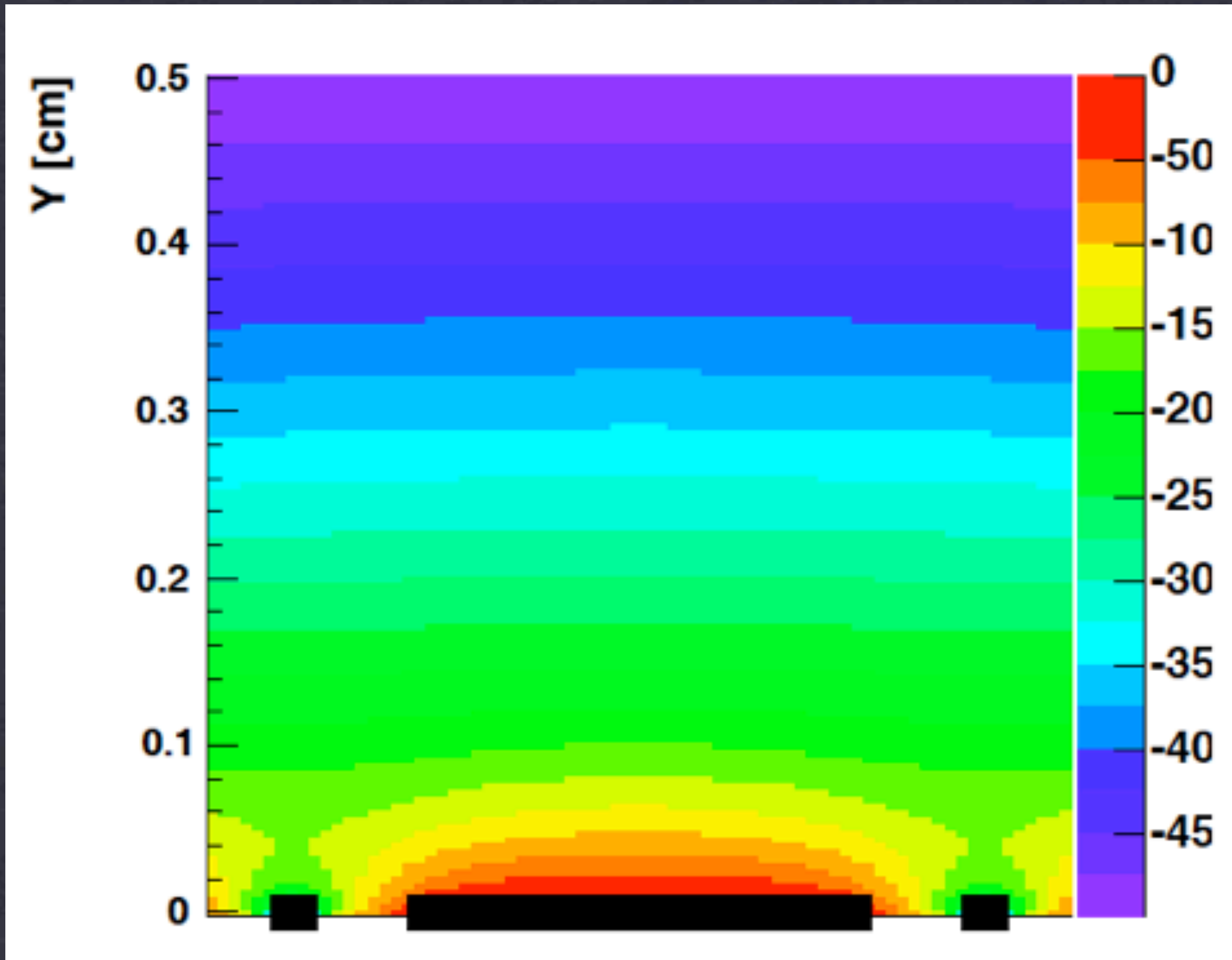

0.5 cm thick CZT, -1000 V bias:

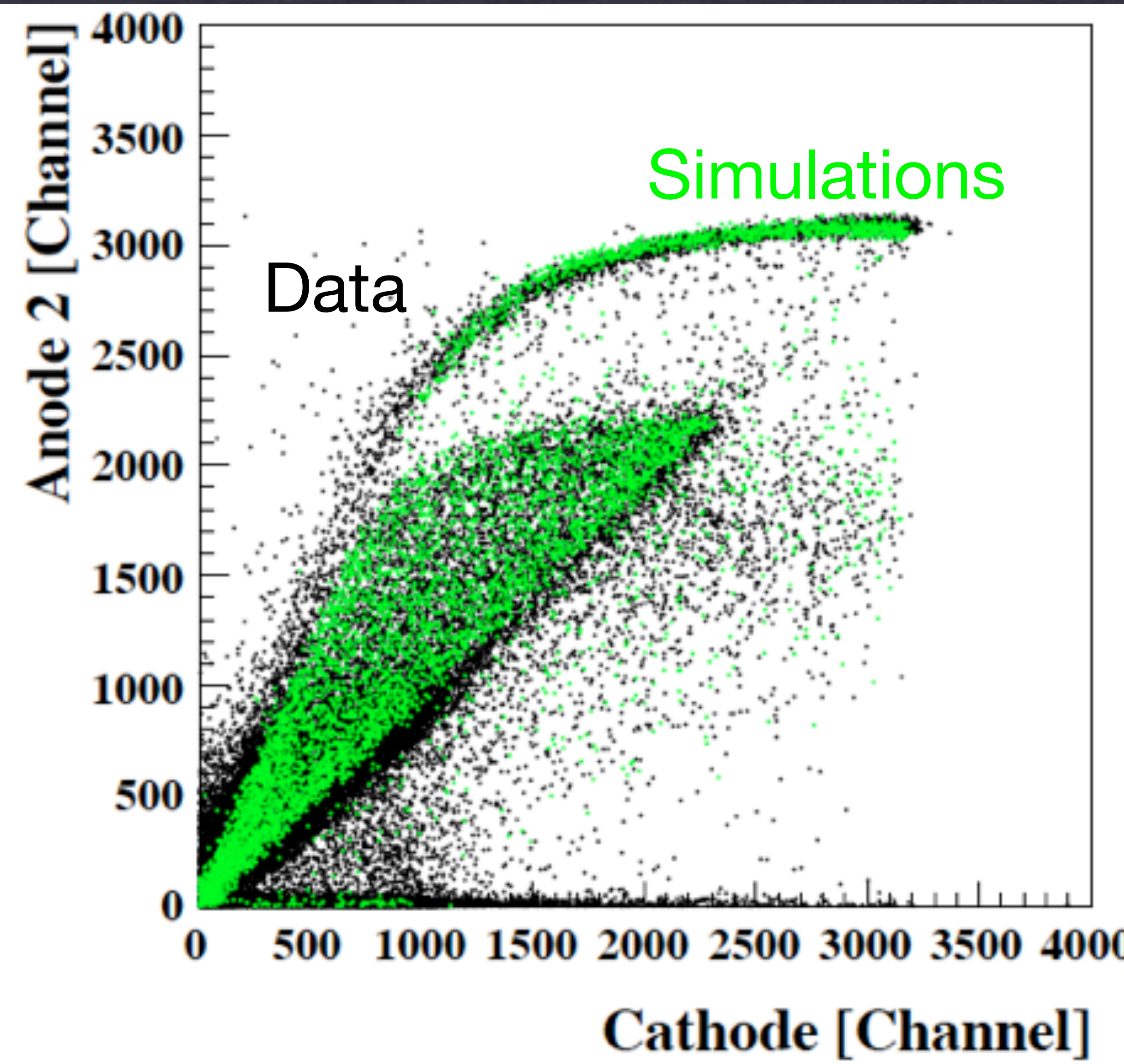

- $\mu_e = 700$ cm^2 V^{-1} s^{-1} , $\tau_e = 5.9 \times 10^{-6}$ s;
- $\mu_h = 50$ cm^2 V^{-1} s^{-1} , $\tau_h = 10^{-6}$ s.

Beilicke et al. 2012

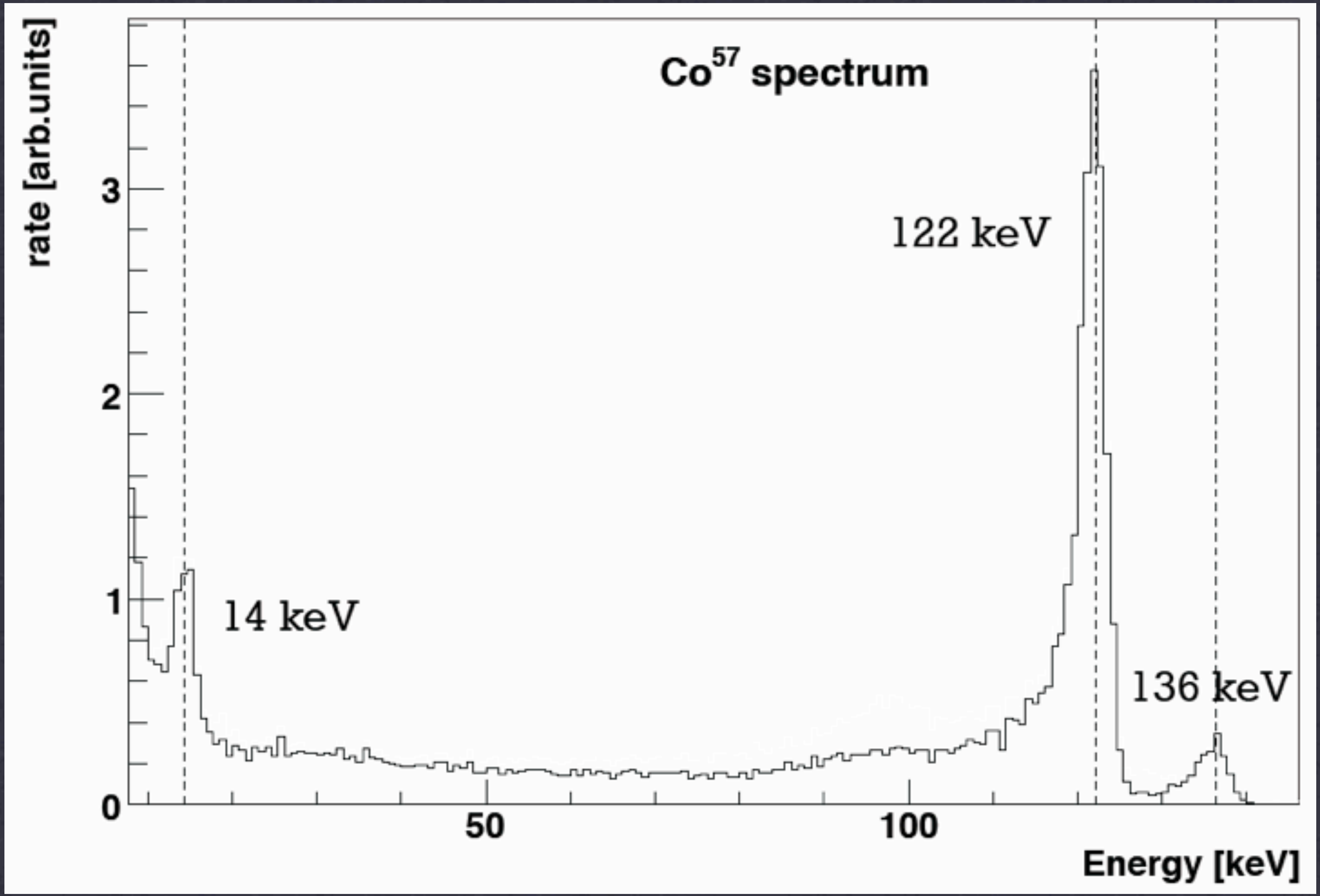

Orbotech CZT, 0.5x2x2 cm^3

Results: ^{57}Co spectrum after threshold minimization.

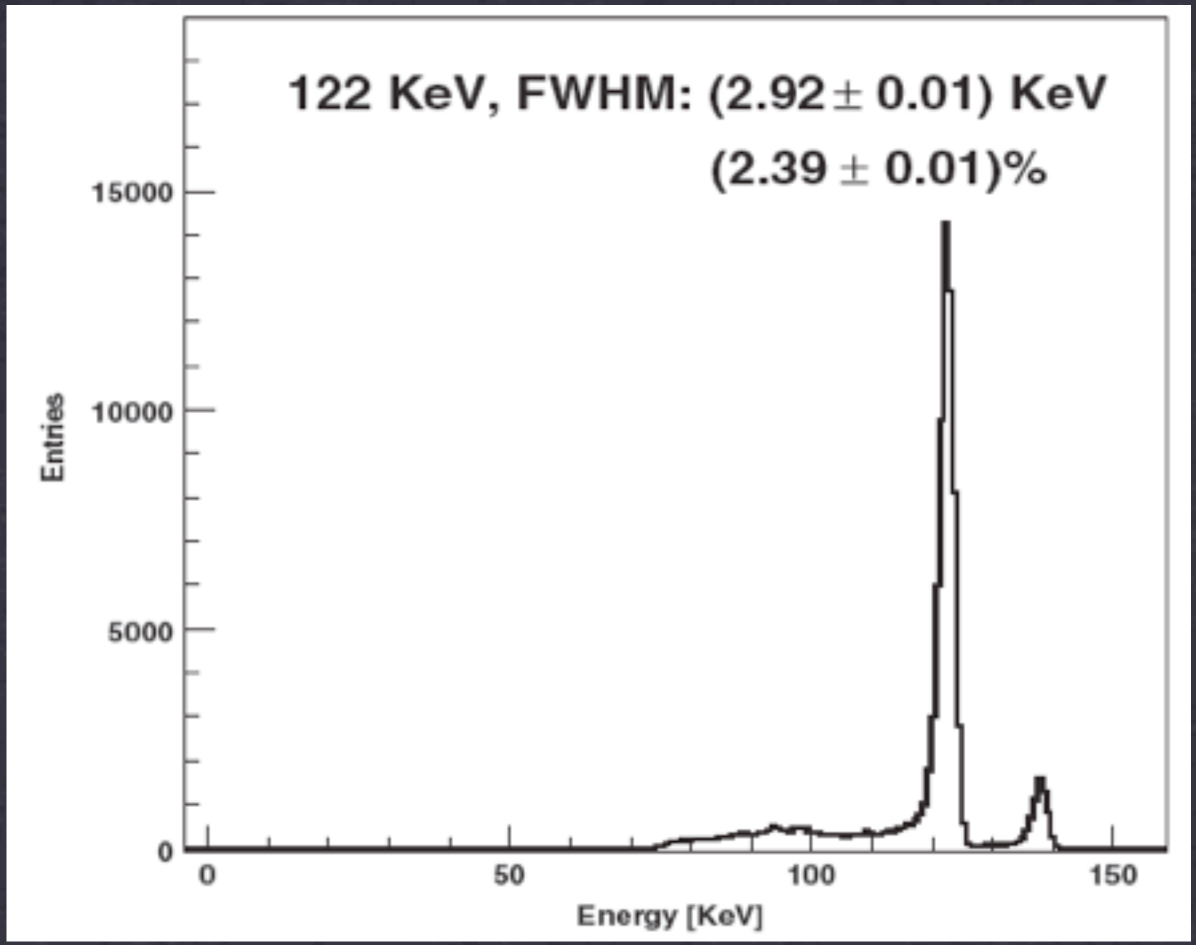

Li et al. 2010

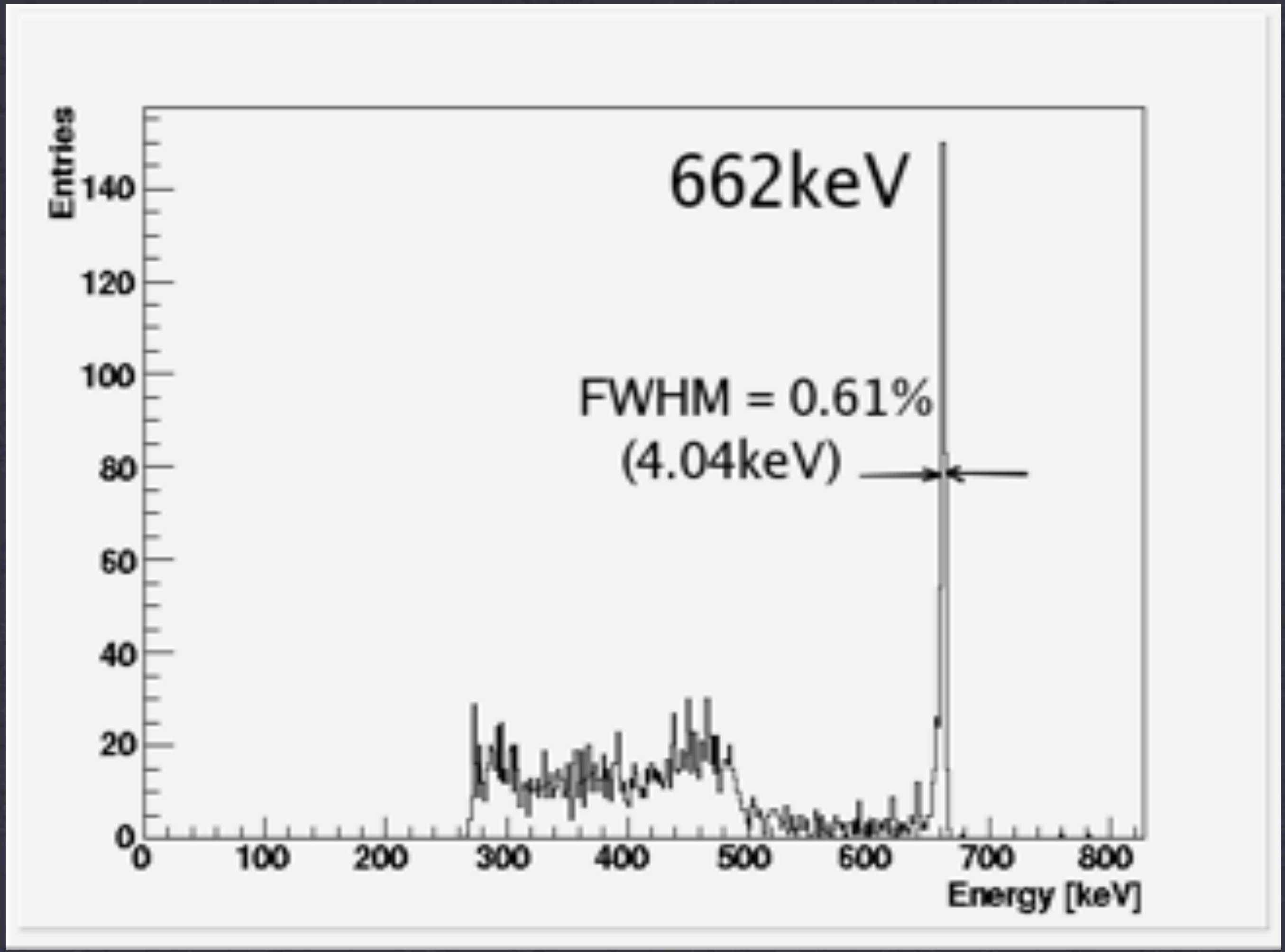

Energy Resolutions (1x2x2 cm^3 eV-Products CZT)

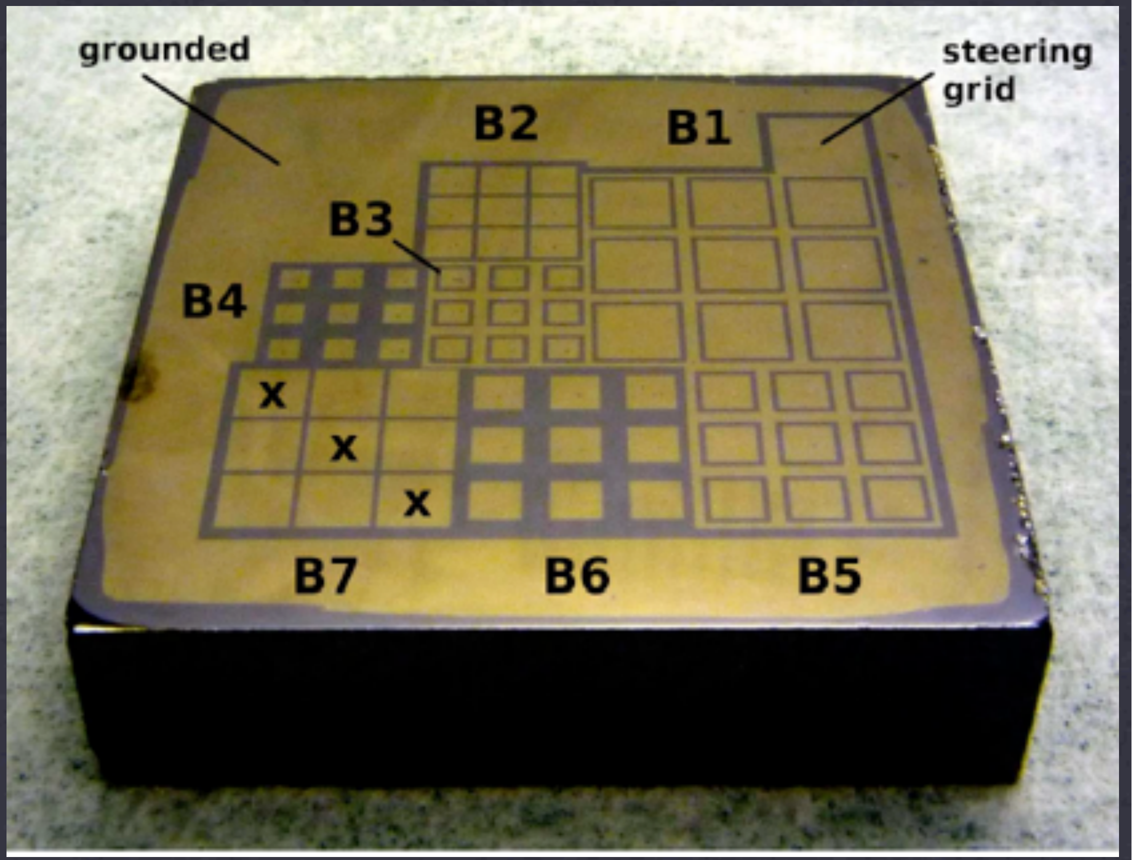

Beilicke et al. 2012

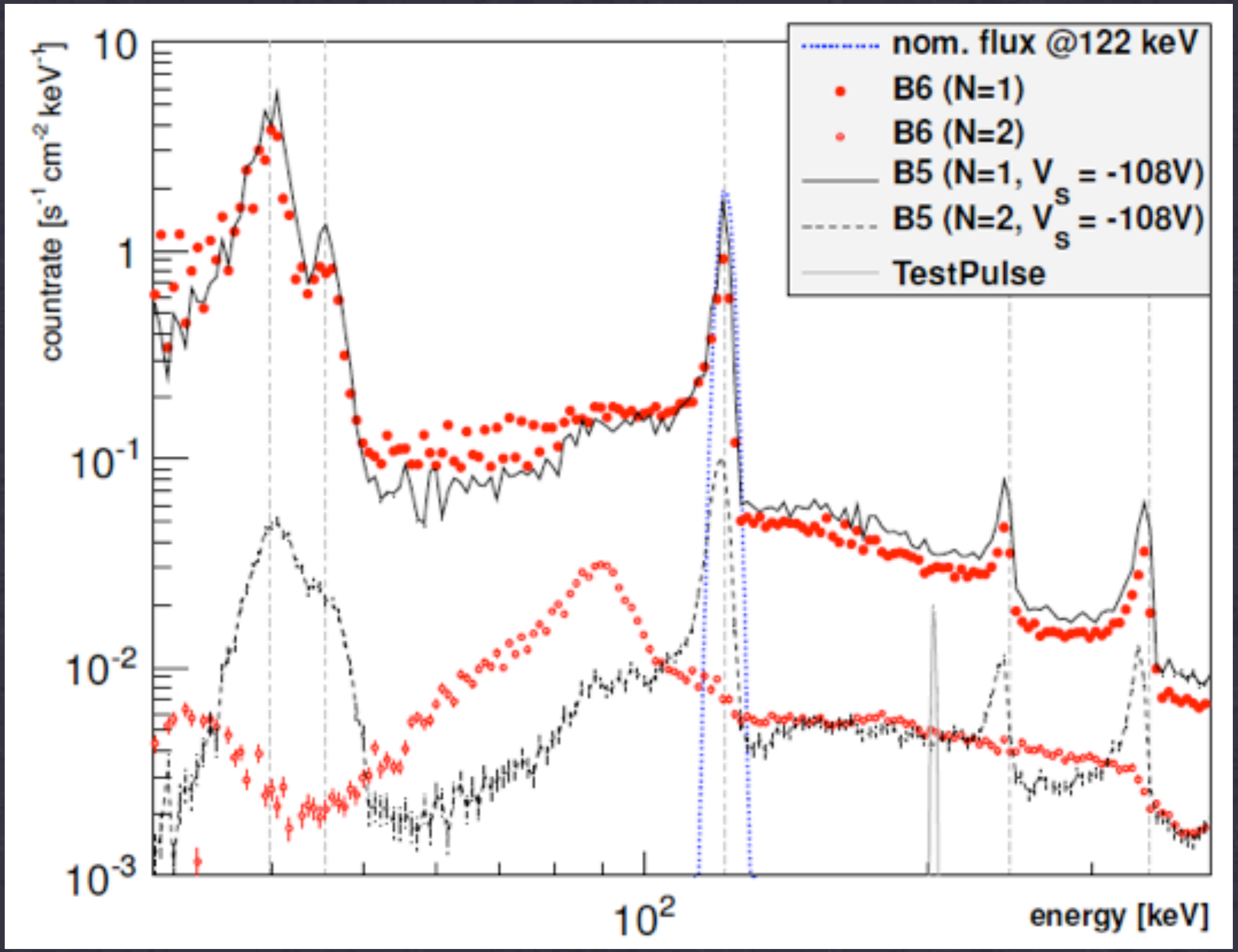

Steering grids improve performance!

Direct Comparison of Different Anode Patterns

CZT Based Astroparticle Physics Experiments

Experiment	Start	Number of Detectors	Volume of Detectors	Pixels per Detector	Energy Range
Swift (BAT)	2004	32,768	0.2x0.4x0.4 cm^3	1	15-150 keV
NuSTAR	2012	4	0.2x1.9 x1.9cm^3	1024	5-80 keV
X-Calibur	2013	32	0.2x2x2cm^3 0.5x2x2cm^3	64	20-70 keV
COBRA	tbd	9,556	0.5x4x4cm^3	256	2-3 MeV

The SWIFT Burst Alert Telescope

Barthelmy et al. 2005

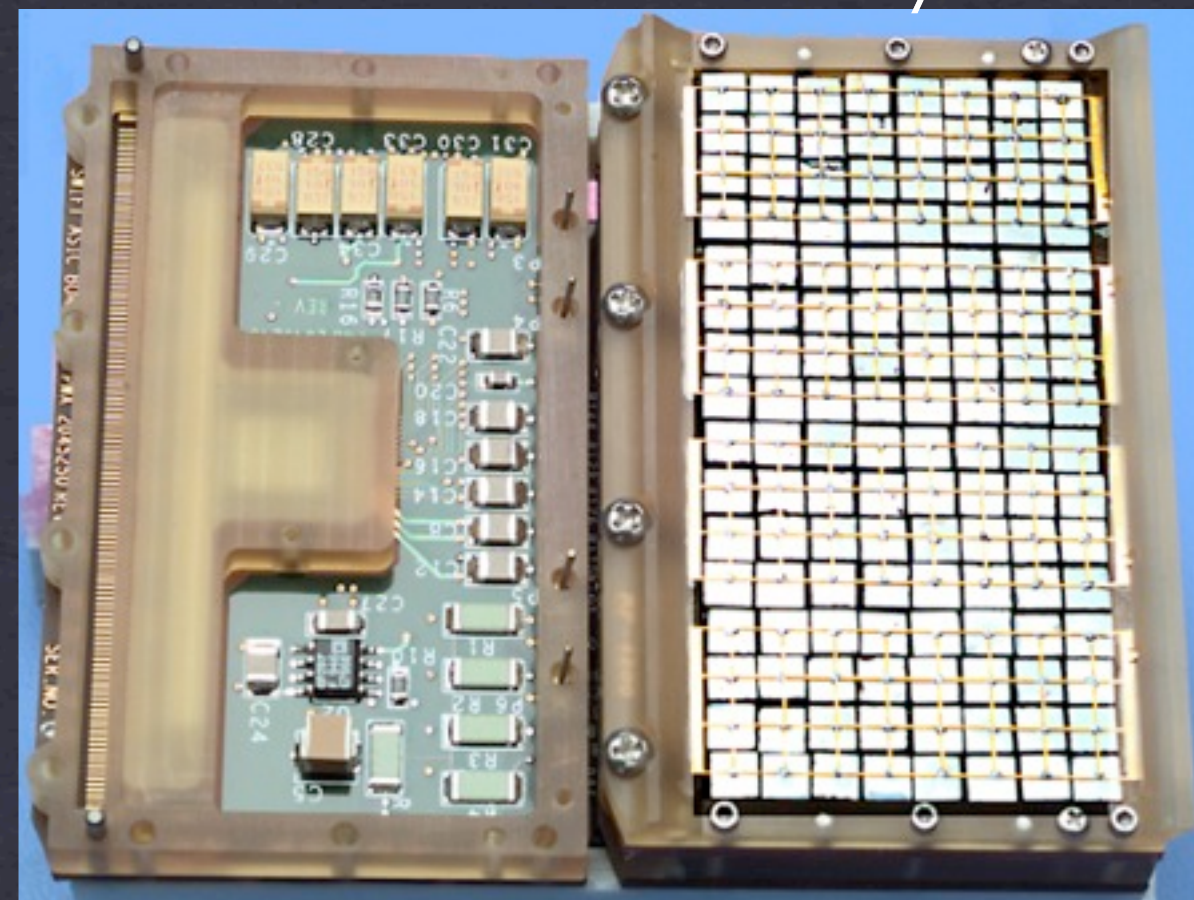

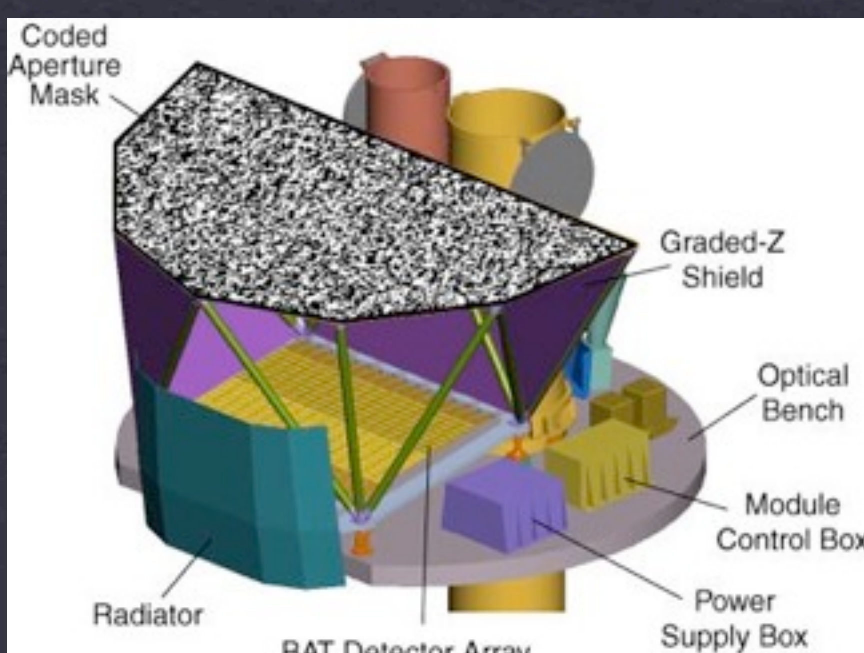

Property	Description
Aperture	Coded mask
Detecting Area	5200 cm^2
Detector	CdZnTe
Detector Operation	Photon counting
Field of View	1.4 sr (partially-coded)
Detection Elements	256 modules of 128 elements
Detector Size	4 mm x 4 mm x 2mm
Telescope PSF	17 arcmin
Energy Range	15-150 keV

The SWIFT Burst Alert Telescope

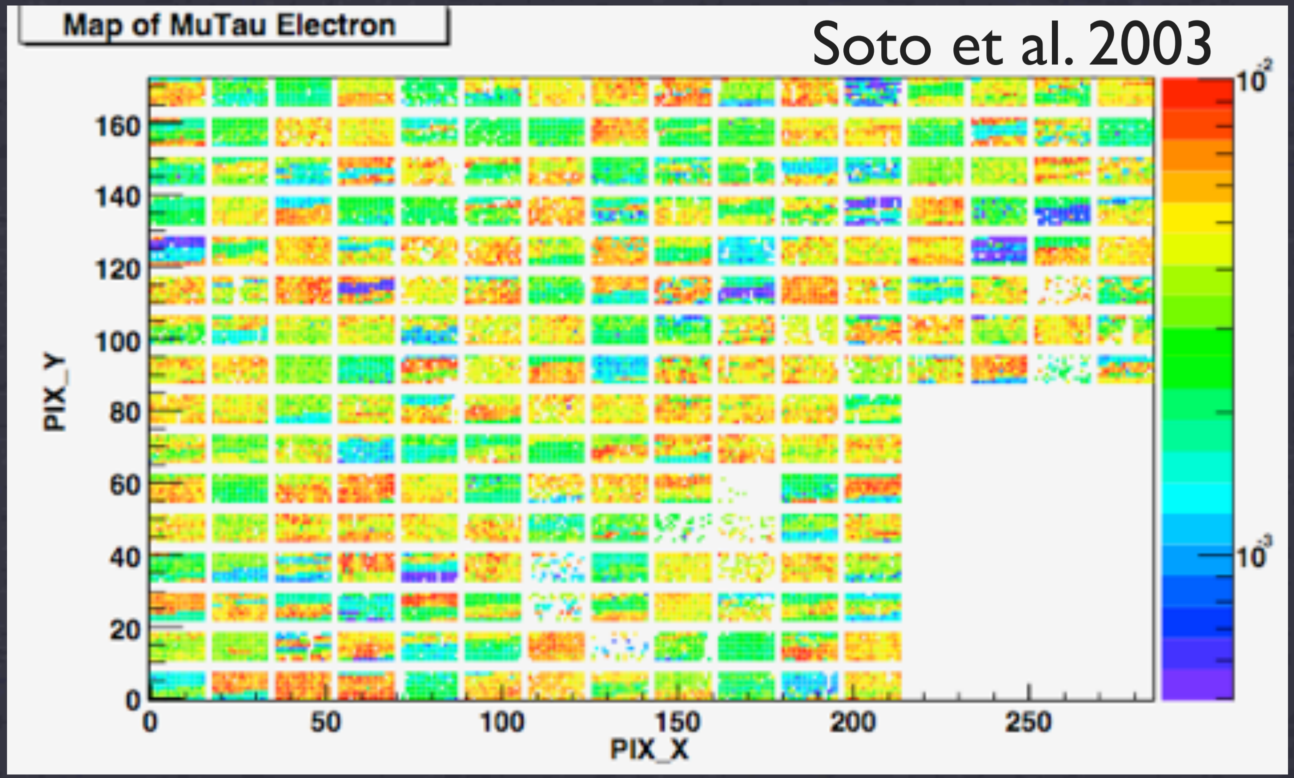

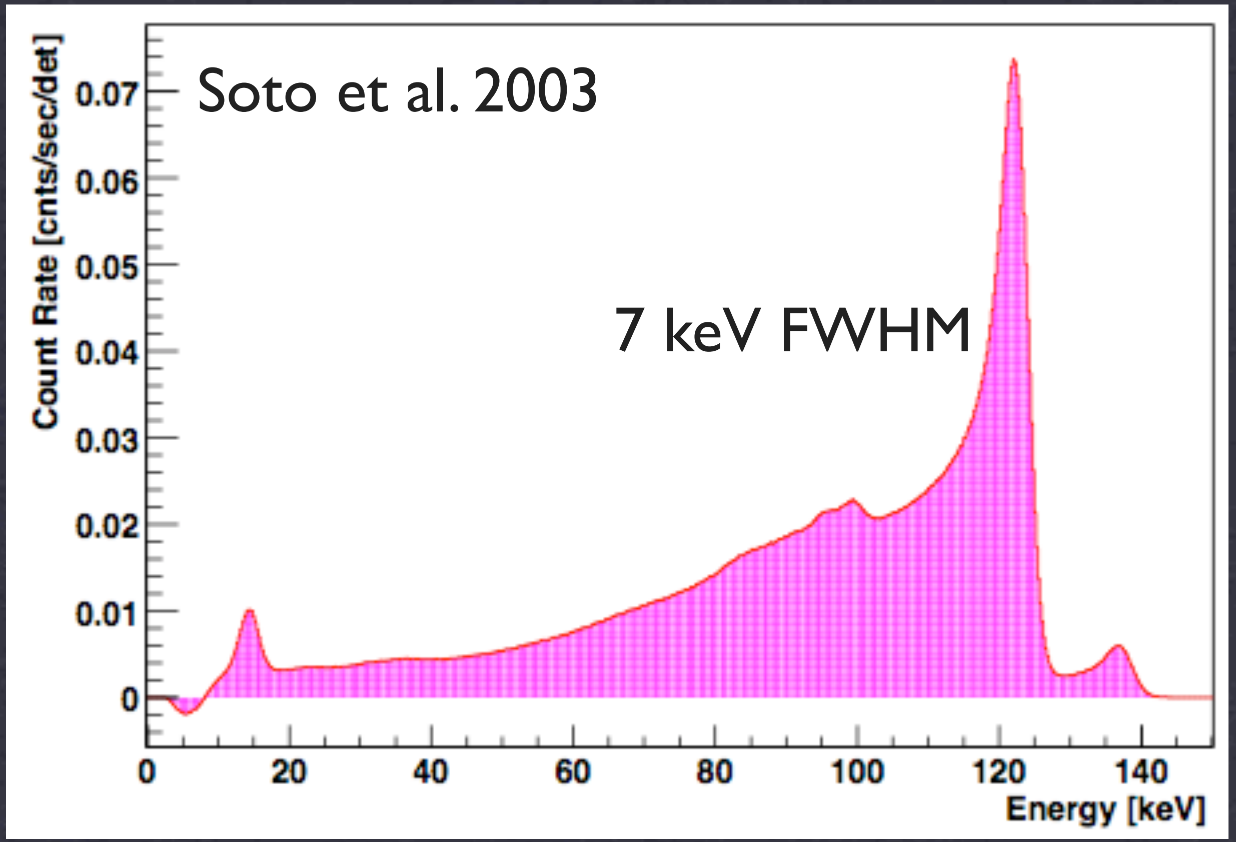

The Nuclear Spectroscopic Telescope Array NuSTAR

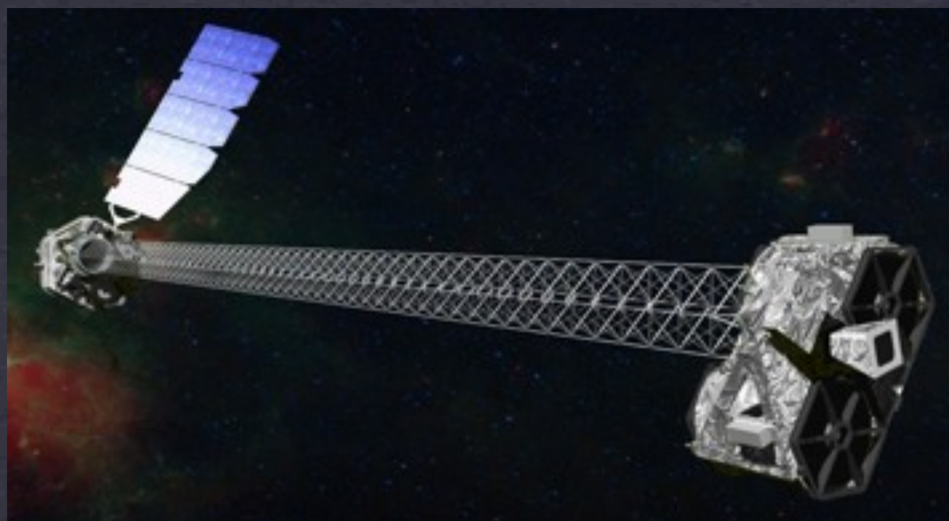

Parameter	Value	Parameter	Value
Pixel size	0.6 mm/12.3″	Max processing rate	400 evt/s
Focal plane size	13′ × 13′	Max flux meas. rate	10^4/s
Pixel format	32 × 32	time resolution	2μsec
Threshold	2.5 keV (each pixel)	Dead time fraction (weak source)	2%

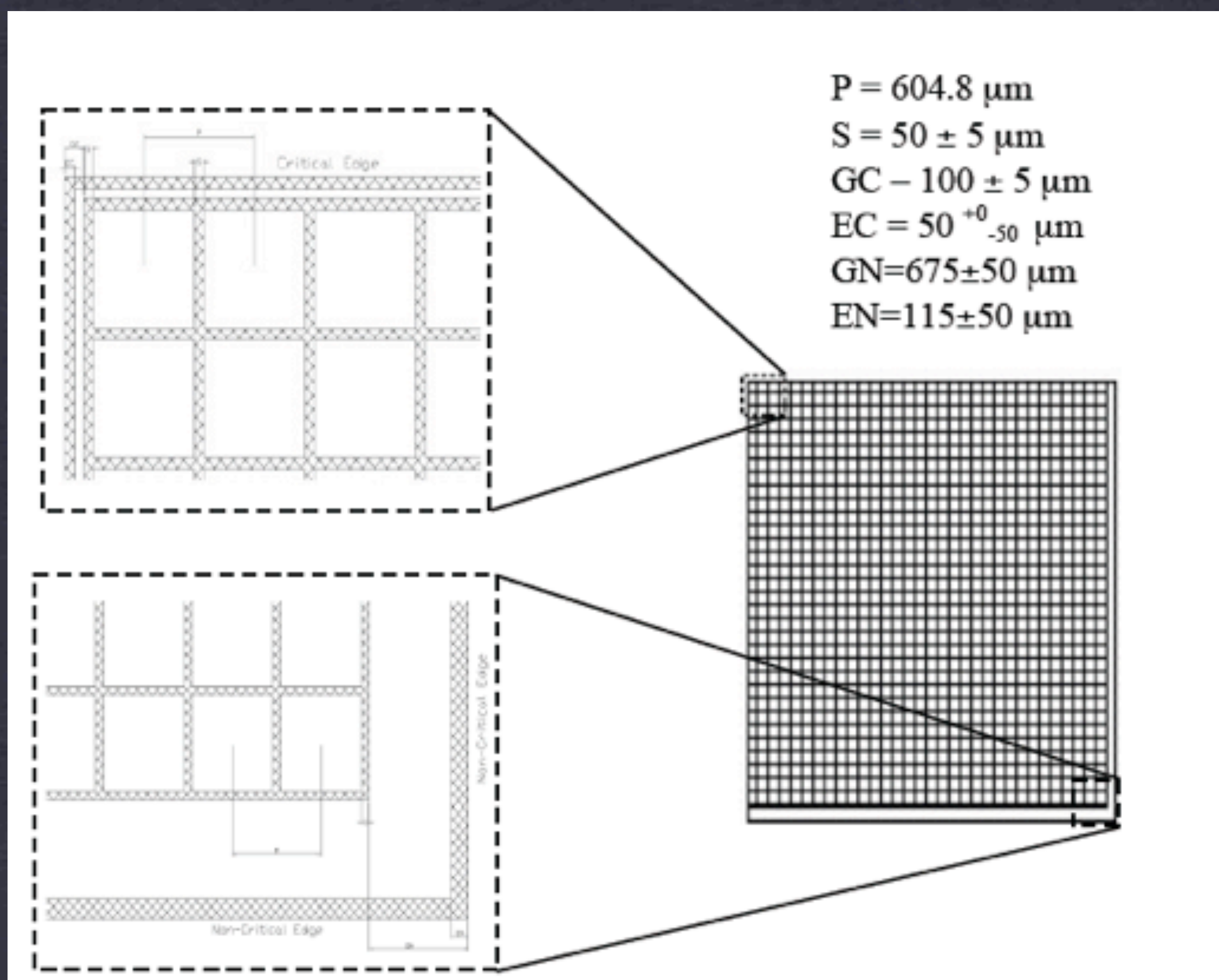

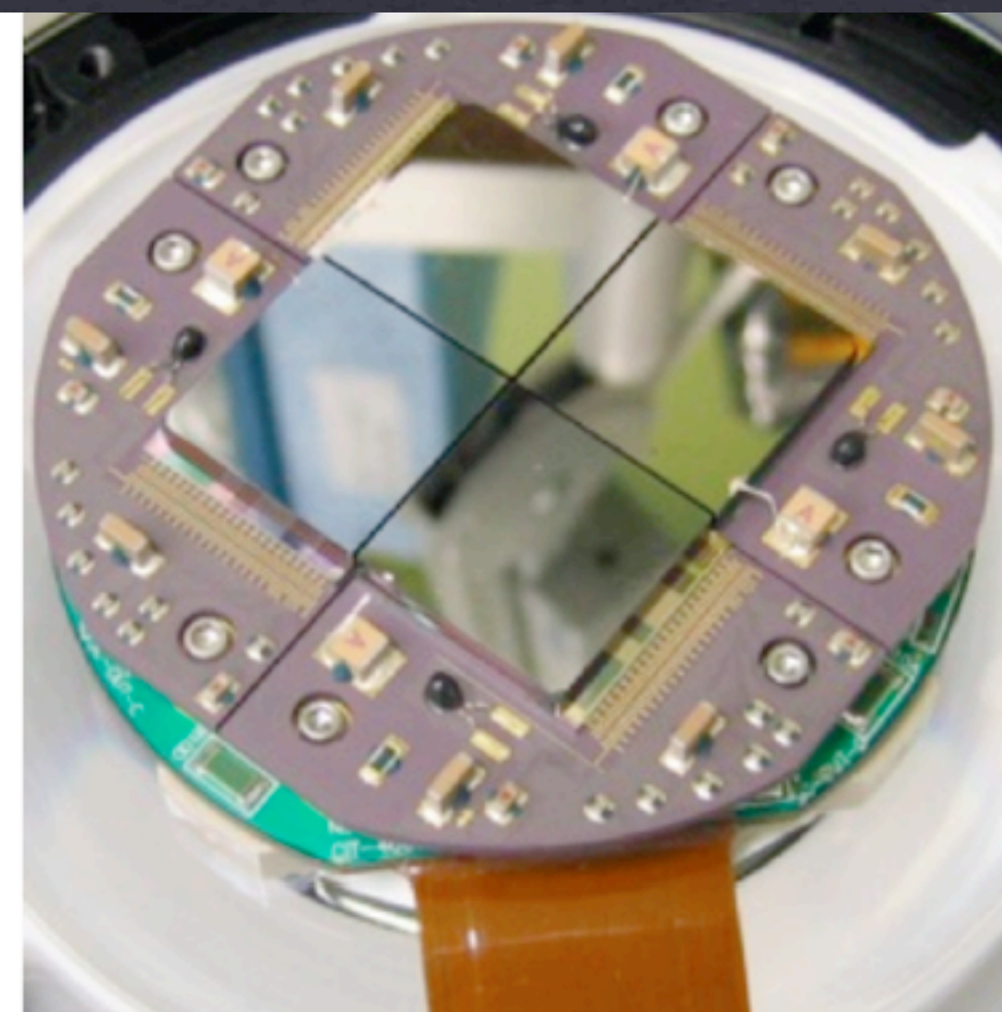

Harrison et al. 2010

The Nuclear Spectroscopic Telescope Array NuSTAR

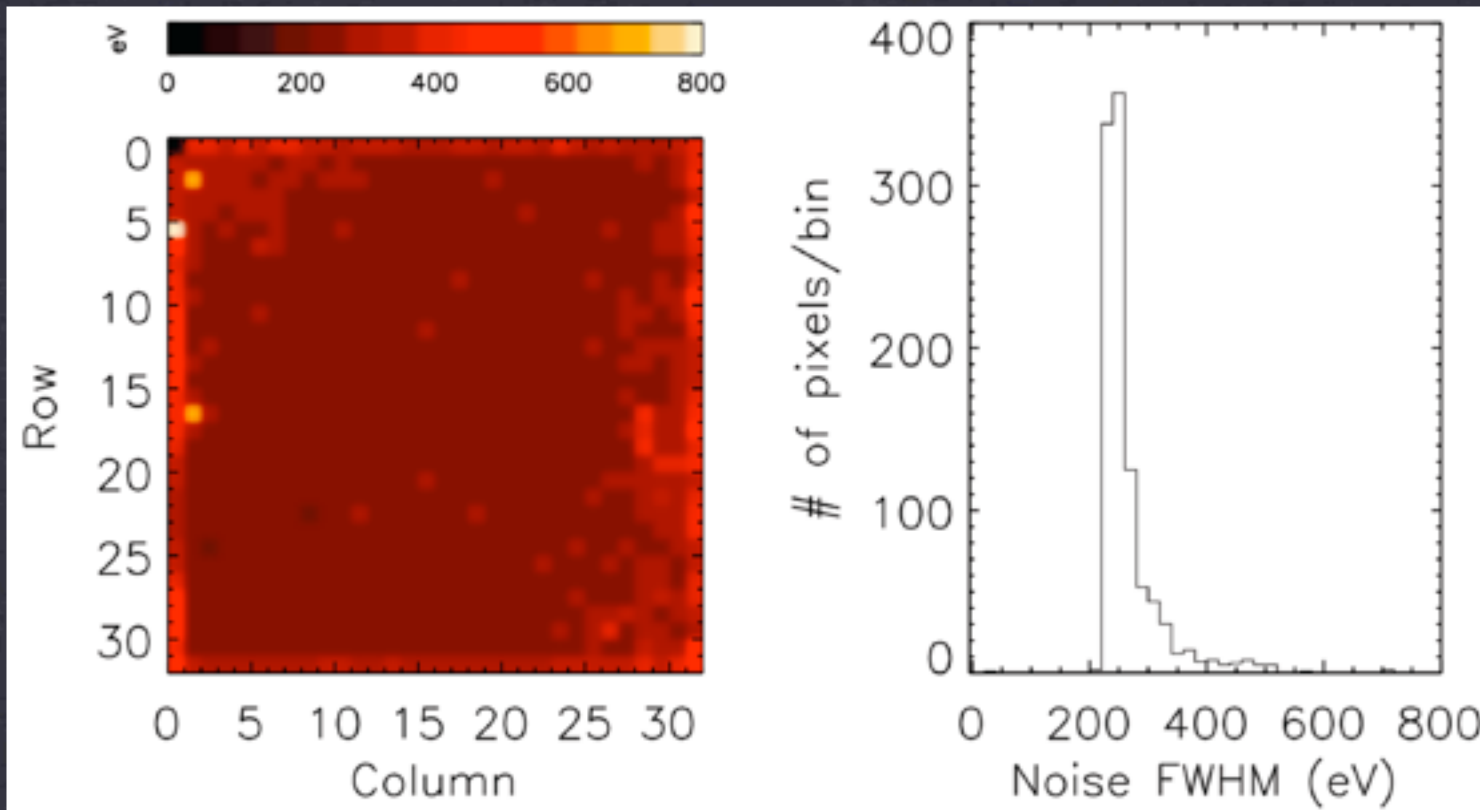

Electronic Noise.

Rana et al. 2009

Detector resolution.

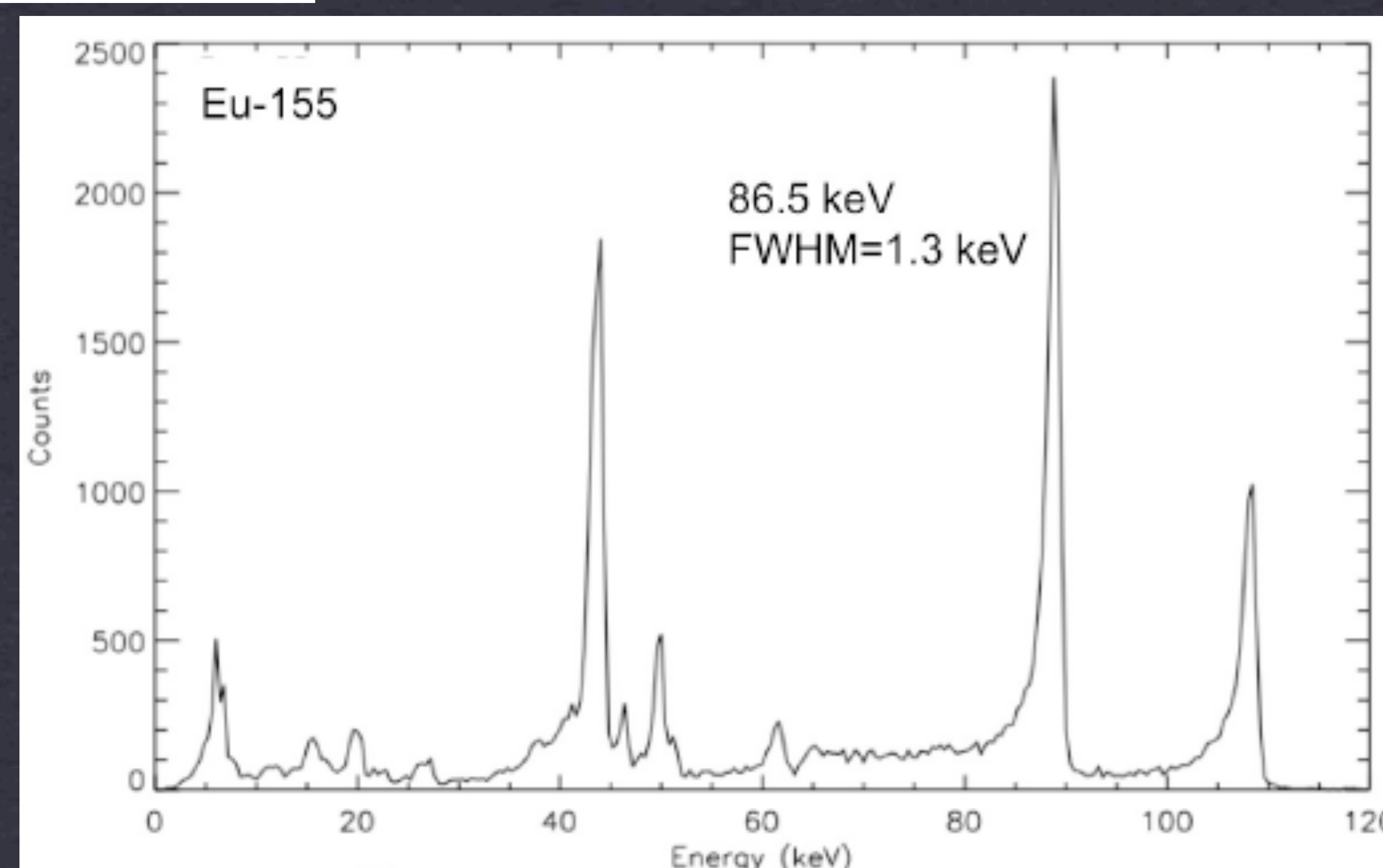

Summary

- In Astrophysics CZT has become the material of choice for the detection of hard X-rays (5 keV - 1 MeV) with excellent spatial and energy resolutions.
- Infrared imaging and Pockels studies show that CZT crystals exhibit a wide range of non-uniformities. Even some good detectors show horizontal E-field variations.
- Thick (>2mm) detectors work best with small pixels.
- Main effect of steering grids: improvement of detection efficiency by ~20%.
- Excellent energy resolutions require small pixels, and thus a considerable number of readout channels.
- Not covered here: COBRA (Zuber et al.), protoEXIST (Grindley et al.) and 3-D CZT time projection detectors (He et al.).